JACS
JOURNAL OF THE AMERICAN CHEMICAL SOCIETY

ARTICLE

pubs.acs.org/JACS

Pd-Catalyzed Copolymerization of Methyl Acrylate with Carbon Monoxide: Structures, Properties and Mechanistic Aspects toward Ligand Design

Akifumi Nakamura,[†] Kagehiro Munakata,[†] Shingo Ito,[†] Takuya Kochi,[†,‡] Lung Wa Chung,[§] Keiji Morokuma,[*,§] and Kyoko Nozaki[*,†]

[†]Department of Chemistry and Biotechnology, Graduate School of Engineering, The University of Tokyo, 7-3-1 Hongo, Bunkyo-ku, Tokyo 113-8656, Japan

[§]Fukui Institute for Fundamental Chemistry, Kyoto University, Takano-Nishishiraki-cho, 34-4, Sakyo-ku, Kyoto 606-8103, Japan

Supporting Information

ABSTRACT: Full details are provided for the alternating copolymerization of acrylic esters with carbon monoxide (CO) catalyzed by palladium species bearing a phosphine−sulfonate bidentate ligand. The copolymer of methyl acrylate (MA) and CO had complete regioregularity with stereocenters that slowly epimerize in the presence of methanol. In the presence of ethylene, terpolymers of MA/ethylene/CO were also prepared. The glass transition temperatures of the co- and terpolymers were higher than that of the ethylene/CO copolymer. Both experimental and theoretical investigations were performed to clarify the superior nature of the palladium phosphine−sulfonate system compared to an unsuccessful conventional palladium diphosphine system: (i) The reversible insertion of CO was directly observed with the isolated alkylpalladium complexes, [{*o*-((*o*-MeOC$_6$H$_4$)$_2$P)C$_6$H$_4$SO$_3$}PdCH(CO$_2$Me)CH$_2$COMe], whereas it was not observed with the corresponding complex bearing 1,2-bis(diphenylphosphino)ethane (DPPE). (ii) The transition state of the subsequent MA insertion, the rate-determining step of the catalytic cycle, was lower in energy in the phosphine−sulfonate system than in the DPPE system. This stabilization could be attributed to the less hindered sulfonate moiety as well as the stronger back-donation from palladium to the electron-deficient olefin, which is located *trans* to the sulfonate.

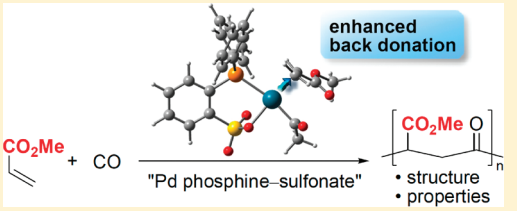

INTRODUCTION

γ-Polyketones obtained by metal-catalyzed alternating copolymerization of olefins with carbon monoxide (CO) have attracted much attention from academic and industrial communities.[1,2] This is because CO is an inexpensive resource and the resulting copolymers exhibit unique properties, such as high crystallinity and photodegradability. Potential industrial applications of the polyketones include fibers, film coatings, adhesives, membranes, and packaging materials.[3] Furthermore, the reactive carbonyl groups in the polymer backbone can be chemically modified and, thus, the polyketones serve as excellent starting materials for other types of functionalized polymers.[4]

The properties of the copolymers can be tuned by changing the olefinic comonomers. Thus far, monosubstituted alkenes such as propylene and styrene derivatives have been well documented as comonomers for copolymerization with CO.[1] A variety of functionalized olefins whose functional groups are separated from the olefin moiety by at least one methylene spacer are also available for copolymerization (Scheme 1).[5,6] In sharp contrast, the copolymerization of fundamental polar monomers with carbon monoxide has been a long-standing challenge in polymer chemistry.[7,8] The fundamental polar vinyl monomers[9] such as methyl acrylate (MA), vinyl acetate, and vinyl chloride are inexpensive and readily available. The resulting copolymers would possess functional groups directly attached to the polymer main chain and their properties are expected to be quite different from ethylene/CO copolymers.

Especially in the case of MA, the possibility of copolymerization with CO has been well studied for complexes ligated by several types of ligands shown in Scheme 2.[7] It had been postulated that no reaction occurred following the formation of **III** (or further reaction was not described), generated by the insertion of CO into the Pd−Me bond of **I** and the subsequent insertion of MA into the Pd−COMe bond of **II**. The resulting five-membered chelate complexes (**III**) were found to be inactive toward further insertion of CO and/or MA.

In 2007 and 2008, we found that vinyl acetate/CO[10] and MA/CO[11] can be copolymerized when a mixture of phosphonium−sulfonate salt **1** and a Pd(0) source was employed as a catalyst. In the case of MA, it was shown that the isolated Pd(II) complex **3a** bearing a phosphine−sulfonate ligand, corresponding to **III** in Scheme 2, also successfully initiates the copolymerization. The series of Pd phosphine−sulfonate complexes, the catalysts we

Received: January 13, 2011
Published: April 11, 2011

ACS Publications © 2011 American Chemical Society

dx.doi.org/10.1021/ja2003268 | *J. Am. Chem. Soc.* 2011, 133, 6761–6779

Scheme 1. Reported Functionalized γ-Polyketones

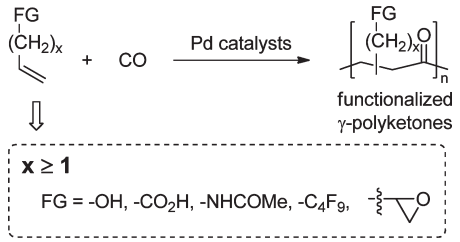

Scheme 2. Reported Inactive Pd Complexes for Copolymerization of Methyl Acrylate with Carbon Monoxide

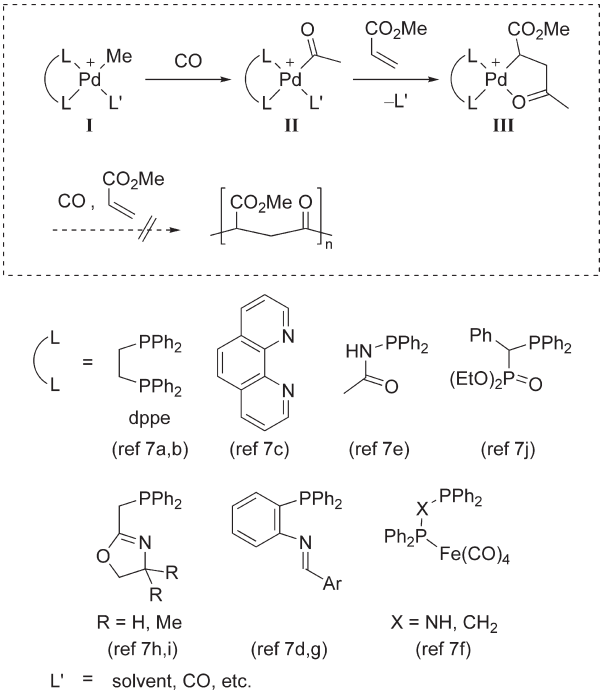

used, have been recently recognized as potent catalysts for coordination copolymerization of ethylene with polar vinyl monomers since their first academic report by Drent in 2002.[1h,9c,12,13] These polyethylenes possessed highly linear structures[14] with functional groups directly attached to the linear polyethylene chain, which has not been obtained by any other catalysts. Furthermore, Pd phosphine−sulfonate catalysts can produce nonalternating ethylene/CO copolymers, which are not accessible by Pd catalysts with conventional diphosphine or diamine ligands.[15,16] For the past decade, the Pd phosphine−sulfonate complexes have conquered a considerable number of challenging problems in polymer chemistry. Nevertheless, the reasons for the success are still unclear. Specifically, a reasonable understanding of how the unique design of the ligand contributes to the successful and unprecedented copolymerization of polar monomers is needed.

This article presents the details of this unprecedented alternating copolymerization of MA with CO catalyzed by Pd phosphine−sulfonate catalysts. The main aim of this study is to reveal the role of the sulfonate moiety in the catalyst through comparison with conventional ligands. The contents of this report are in the following order. The details of the syntheses (Section 1) and the structural analyses (Section 2) of acrylates/CO copolymers are disclosed. Terpolymers of MA/ethylene/CO were also obtained and characterized (Section 3). In addition, the thermal properties of these co- and terpolymers were investigated (Section 4). Subsequently, the mechanism of the MA/CO copolymerization was investigated experimentally (Section 5) and theoretically (Section 6) to clarify why the Pd phosphine−sulfonate complex catalyzed the copolymerization while the other catalysts could not (Section 7).

RESULTS AND DISCUSSIONS

1. Copolymerization of Acrylates with Carbon Monoxide. The alternating copolymers of MA with CO were obtained using catalysts generated *in situ* from $Pd(dba)_2$ and phosphonium−sulfonate **1**.[11] Treatment of MA with 6.0 MPa of CO at 70 °C for 20 h in the presence of $Pd(dba)_2$/**1a** afforded the copolymer with M_n of 30 000 (white solid after reprecipitation, see Experimental section, entry 1, Table 1).[17,18] *o*-Methoxyphenyl substituted ligand **1a** offers both higher activity and molecular weights of the copolymers than the phenyl substituted **1b** (entries 1 and 2). It should be noted that the reaction using cyclohexyl substituted ligand $(Cy_2PH)C_6H_4SO_3$[12h] or 2-(diphenylphosphino)benzoic acid did not afford the copolymer. When 2 equiv of ligand **1a** were used, the activity was decreased (entry 3). This tendency was also observed in the copolymerization of ethylene with CO,[15b] suggesting that the initiation with *in situ* formed [P−O]-Pd[P−O] complexes is sluggish.

The activity of the copolymerization was dependent on CO pressure (entries 1, 4 and 5). An increase in CO pressure (up to 8.0 MPa) led to an enhancement in catalytic activity. According to the mechanistic studies in Sections 5 and 6 (*vide infra*), CO coordination−insertion is a reversible, pre-equilibrium step. Thus, the increased activity at higher CO pressure can be interpreted as a result of increased concentration of acylpalladium species, which is advantageous for subsequent MA insertion.

Increasing the reaction temperature from 45 °C (entry 6) to 70 °C (entry 1) substantially enhanced the activity and molecular weight. However, the molecular weight of the copolymer produced at 100 °C (entry 7) decreased while the catalytic activity was similar to that produced at 70 °C. The number of the polymer chains produced per catalyst (P/C) at 100 °C was 2.6, which indicates that the chain transfer reaction (see Section 2) was accelerated as well as the polymerization reaction at high temperature.

To obtain the copolymer with higher molecular weight, a longer reaction time was employed (entry 8). After 144 h, the copolymer with higher molecular weight (M_n 40 000), broader M_w/M_n and low TOF was obtained. In this case, high viscosity of the reaction mixture seems to be the major obstacle to the rapid propagation reaction.

The isolated Pd phosphine−sulfonate complexes were also investigated as catalysts. In the case of 2,6-lutidine-bound complex **2a**, only a trace amount of the copolymer was obtained (entry 9). This result suggests that the strong binding affinity of 2,6-lutidine inhibits the coordination of electron-deficient MA.[19] On the other hand, nitrogen-free complex **3a**, which was prepared by the insertion of one equivalent of MA to acylpalladium complex (**4a**) (Scheme 3), initiated and catalyzed the copolymerization of MA/CO effectively (entry 10).[11]

The copolymerization of a variety of monomers has been examined in addition to MA. *t*-Butyl acrylate can be copolymerized

dx.doi.org/10.1021/ja2003268 |*J. Am. Chem. Soc.* 2011, 133, 6761–6779

Table 1. Copolymerization of Acrylates with Carbon Monoxide[a]

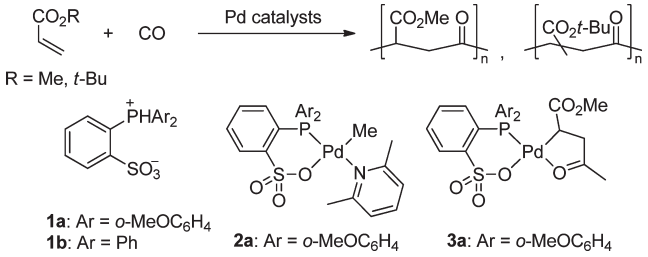

entry	catalyst	R	P_{CO} (MPa)	temp (°C)	time (h)	yield (mg/%)[b]	TOF (h^{-1})	M_n[c] ($\times 10^3$)	M_w/M_n	P/C[d]
1	**1a**/Pd(dba)$_2$	Me	6.0	70	20	490/15	21	30	1.6	1.7
2	**1b**/Pd(dba)$_2$	Me	6.0	70	20	140/4.3	6.0	26	1.2	0.53
3	**1a**[e]/Pd(dba)$_2$	Me	6.0	70	20	260/12	11	6.0	1.3	4.3
4	**1a**/Pd(dba)$_2$	Me	3.0	70	20	370/12	16	21	1.6	1.8
5	**1a**/Pd(dba)$_2$	Me	8.0	70	20	540/17	24	17	1.7	3.4
6	**1a**/Pd(dba)$_2$	Me	6.0	45	20	150/4.8	6.7	16	1.3	1.0
7	**1a**/Pd(dba)$_2$	Me	6.0	100	20	500/16	22	19	1.7	2.6
8	**1a**/Pd(dba)$_2$	Me	6.0	70	144	1500/48	9.2	40	2.0	3.8
9	**2a**	Me	6.0	70	20	43/1.3	1.8	2.1	1.1	2.0
10	**3a**	Me	6.0	70	20	580/18	25	24	1.6	2.4
11	**1a**/Pd(dba)$_2$	*t*-Bu	6.0	70	20	90/3.3	2.9	7.9	1.5	1.1

[a] Unless otherwise noted, reaction was performed with 0.012 mmol of ligand **1**, 0.010 mmol of Pd source, and 2.5 mL of methyl acrylate without additional solvent. [b] Yield of the copolymer was determined by subtraction of the weight of catalyst from the amount of solid product obtained and calculated based on the acrylate used. [c] Molecular weights were determined using narrow polystyrene standards. [d] Number of polymer chains produced per catalyst based on palladium. [e] Two equivalents of ligand **1a** (0.020 mmol) was used.

Scheme 3. Synthesis of Five-Membered Chelate Complex 3a Bearing a Phosphine−Sulfonate Ligand[11]

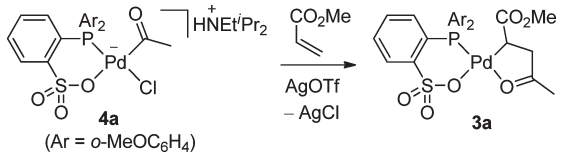

with CO (entry 11) and the regioregularity of the resulting copolymer was not controlled while the copolymerization of methyl acrylate/CO afforded regiocontrolled product (see Section 2). Aside from the acrylates and vinyl acetate,[10] none of the attempted polar vinyl monomers whose olefin moieties are directly functionalized[1h] participated in copolymerization under the conditions of entry 1. Attempted copolymerization of methyl methacrylate with CO resulted in homopolymerization of methyl methacrylate probably via radical pathway.[20] Methyl vinyl ketone, *N*-isopropylacrylamide, acrylonitrile, vinyl chloride did not afford any polymeric products. When we used *N*-vinyl pyrrolidone, only head-to-tail dimer was obtained.[21] A trace amount of cooligomer of *n*-butyl vinyl ether/CO was detected by MALDI-TOF MS spectrum, but the only major product was poly(butyl vinyl ether)[22] as confirmed by NMR.

2. Structural Analyses of the Copolymers of Acrylates with Carbon Monoxide. The microstructure of γ-polyketones is one of the most important factors that affect their physical properties.[1b,e] The regio-, stereo-, and enantiocontrol of γ-polyketones have, thus far, been well investigated for

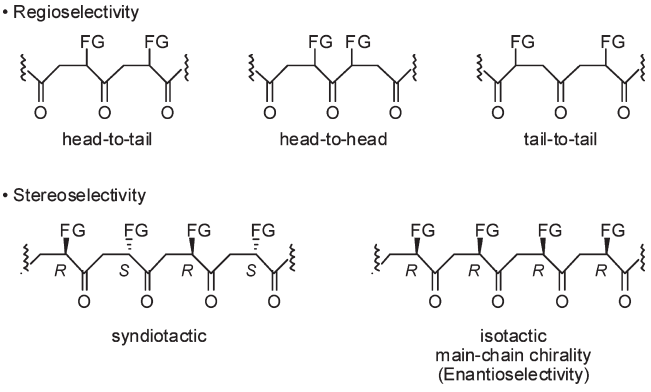

Figure 1. Microstructures in γ-polyketones. FG = $-CH_3$ for poly(propylene-*alt*-CO) and $-CO_2Me$ for poly(methyl acrylate-*alt*-CO).

poly(propylene-*alt*-CO) and poly(styrene-*alt*-CO) (Figure 1). In the previous communication, we confirmed the regiocontrolled, alternating structure of poly(methyl acrylate-*alt*-CO) by NMR and MALDI-TOF mass spectroscopy.[11,23] The exquisite control of head-to-tail architecture was inferred from the observation of only a single singlet resonance in the ketone region in ^{13}C NMR spectrum (Figure 2B).

Although a single resonance was observed in the ketone region at room temperature, it was found to split into multiple peaks at −60 °C (Figure 2C). In addition, the signal is wider than that of regio-, stereo- and enantiocontrolled *iso*-poly(propylene-*alt*-CO) in Figure 2D.[24] Therefore, it was assumed that epimerization at the asymmetric carbon center might occur,

dx.doi.org/10.1021/ja2003268 |J. Am. Chem. Soc. 2011, 133, 6761–6779

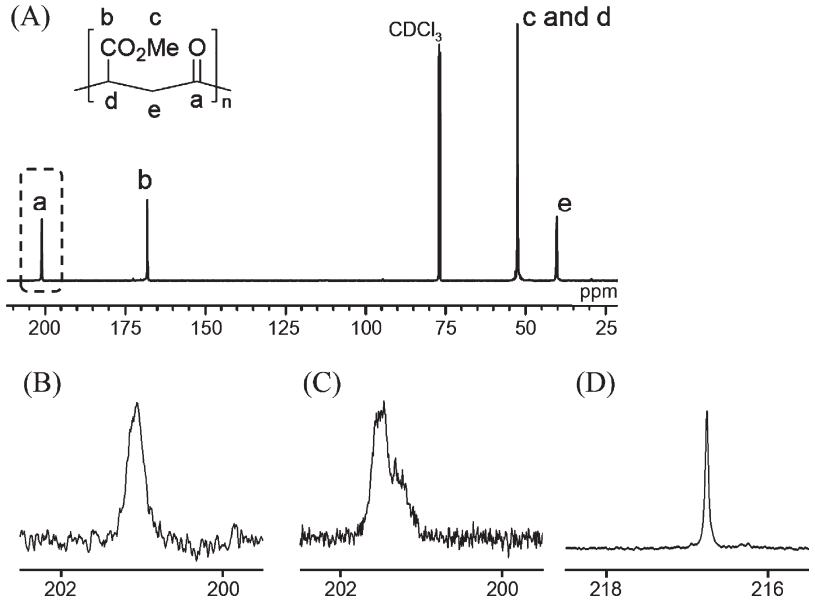

Figure 2. ^{13}C NMR spectra of (A) poly(methyl acrylate-*alt*-CO), (B) the ketone carbonyl region of poly(methyl acrylate-*alt*-CO) at ambient temperature, (C) the ketone carbonyl region of poly(methyl acrylate-*alt*-CO) at −60 °C, and (D) the ketone carbonyl region of isotactic poly(propylene-*alt*-CO).[24]

Scheme 4. H/D Exchange of Methine Protons of Poly(methyl acrylate-*alt*-CO)

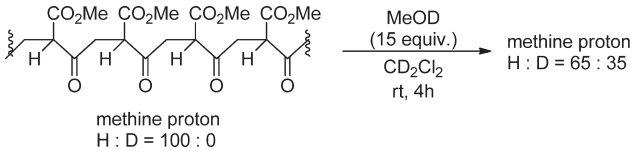

since poly(methyl acrylate-*alt*-CO) is a β-ketoester whose pK_a (≈10) is much lower than that of other γ-polyketones.[25] However, the epimerization rate was found to be too slow to be observed in NMR time scale (10^{-1}−10^{-6} s). When the copolymer was treated with 15 equiv of MeOD (based on the number of repetitive units) in CD_2Cl_2, only 35% of the methine protons were exchanged with deuterium even after 4 h at room temperature (Scheme 4).[26] Thus, the epimerization can occur gradually in the presence of methanol but it does not account for the split of NMR signals in Figure 2C.

According to these results, there are two probable explanations regarding the stereochemistry of poly(methyl acrylate-*alt*-CO). The first possibility is that the stereochemistry is not controlled and the relatively wide NMR signal in Figure 2B is due to the presence of many signals overlapped. In this case, the change of the signal shape at low temperature could be attributed to the restriction of the fluctuation of a high-order structure, for example, helix−coil transition. The second is that the stereochemistry is controlled but the fluctuation of a higher-order structure occurs both at room temperature and at −60 °C.

When *t*-butyl acrylate was used as a monomer (Table 1, entry 11), the signals in the ketone carbonyl region in the ^{13}C NMR spectrum were more complex. The methine protons in the ^{1}H NMR spectrum showed at least three separate signals which indicate the lack of regioselectivity (see Supporting Information).[27] The multiple signals for the ester region (-CO_2*t*-Bu) are within a quite narrow region (168.1−168.4 ppm). The chemical shifts (^{13}C NMR, $CDCl_3$) of isobutyric acid *t*-butyl ester (*i*-PrCO_2*t*-Bu, 176.7 ppm) and isobutyric acid (*i*-PrCO_2H, 184.0 ppm) suggest that the *t*-Bu group of the obtained copolymer is intact.

Scheme 5. Initiation Chain End Analysis of the Copolymers Initiated by (a) the Mixture of 1 and Pd(dba)$_2$ and (b) Isolated Complex 3a[11]

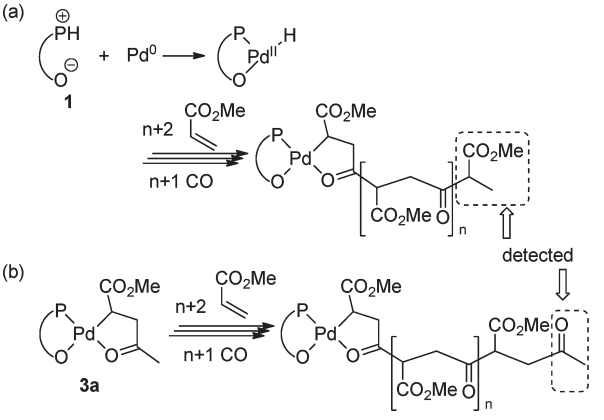

Initiation chain ends of the poly(MA-*alt*-CO) were characterized by ^{1}H NMR spectroscopy and the structures were confirmed as shown in Scheme 5.[11] When a mixture of **1** and Pd(dba)$_2$ was used, a 1-methoxycarbonylethyl group was detected as an initiating chain end, which suggests that the reaction was initiated by the formation of a Pd−H bond via protonation of Pd(0) species,[1h,12a] followed by subsequent insertion of MA and CO. In contrast, copolymers formed with **3a** showed a signal corresponding to the acetyl initiating end group, which originated from the complex **3a** (Scheme 5b).

In the cases where the *P*/*C* values in Table 1 are larger than 1, chain-transfer reactions are suggested to take place during the polymerization, but the structures of terminating chain ends for these polymers could not be identified.[11]

dx.doi.org/10.1021/ja2003268 |*J. Am. Chem. Soc.* 2011, 133, 6761–6779

Table 2. Terpolymerization of Methyl Acrylate/Ethylene/CO[a]

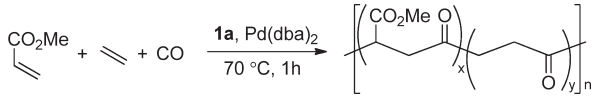

entry	$P_{ethylene}$ (MPa)	P_{total} (MPa)	yield (mg)[b]	activity ($g \cdot mmol^{-1} \cdot h^{-1}$)	x:y	M_n ($\times 10^3$)	M_w/M_n
1[c]	2.0	5.5	80	2.4	11:89	n.d.[b]	n.d.[b]
2[d]	0.5	6.0	45	0.68	45:55	3.1	1.9

[a] Reactions were performed with 0.012 mmol of ligand **1**, 0.010 mmol of Pd source, and 2.5 mL of methyl acrylate without additional solvent. The yield (mg) of the terpolymer was determined by subtraction of the weight of catalyst from the amount of solid product obtained. [b] Molecular weight was not determined due to the low solubility of the ethylene-rich terpolymer in common solvents for SEC analyses. Note that the NMR spectra of this terpolymer were collected in a mixture of $CDCl_3$/1,1,1,3,3,3-hexafluoro-2-propanol (1:2). [c] Ratio of x:y was based on ^{1}H NMR analysis. [d] Ratio of x:y was based on the carbonyl signals in the ^{13}C NMR spectrum.

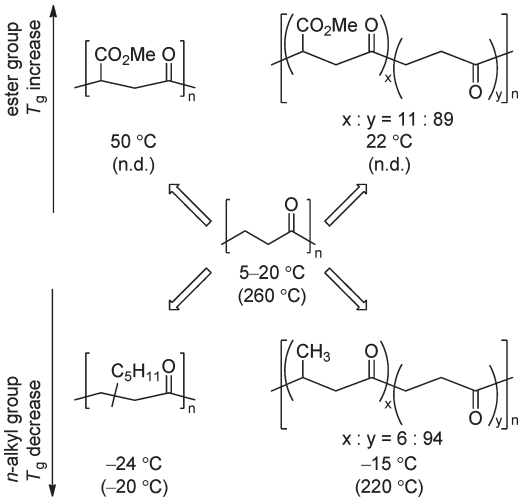

Figure 3. Comparison of the glass transition temperatures (T_g) of the γ-polyketone. The values in parentheses are melting temperatures (T_m). n.d. = not detected.

3. Syntheses and Characterization of Terpolymers of Methyl Acrylate/Ethylene/CO. A mixture of ligand **1a** and $Pd(dba)_2$ catalyzes terpolymerization of MA, ethylene and CO (Table 2).[28,29] The incorporation ratio of the resulting terpolymers depends upon the ethylene pressure. When 2.5 MPa of ethylene was introduced, ethylene-enriched terpolymer was obtained with the ratio of MA and ethylene (x:y) to be ca. 11:89 in a mixture of $CDCl_3$/1,1,1,3,3,3-hexafluoro-2-propanol (1:2) (entry 1, Table 2). In the obtained terpolymers, olefins and CO are aligned in an alternating fashion without any successive olefin moieties.[15,16] In addition, no successive "methyl acrylate-CO" units described as "x" in Table 2 was detected. This is based on the fact that the signals around 201 ppm and 168 ppm, which are the signals for ketone and ester carbonyls in the copolymer, were not detected and other detectable signals in the carbonyl region were all assigned (see Supporting Information).

By decreasing ethylene pressure to 0.5 MPa, the ratio changed to approximately x:y = 45:55 (entry 2, Table 2). However, a detailed assignment of the polymer microstructure was difficult due to its highly complex NMR signals, suggesting a random architecture of the copolymer.

4. Thermal Properties of Co- and Terpolymers. Thermal analyses were carried out for the obtained co- and terpolymers (Figure 3). According to the differential scanning calorimetry (DSC) analyses, T_g of the copolymer of entry 1 in Table 1 (poly(MA-*alt*-CO)) and the terpolymer of entry 2 in Table 2 (poly(CO-*alt*-(ethylene; MA)) were found around 50 °C[11,29] and 22 °C, respectively. These values are higher than that of poly(ethylene-*alt*-CO) (5−20 °C).[1b] This is in a sharp contrast to the *n*-alkyl substituted γ-polyketones, which exhibit lower T_g than that of poly(ethylene-*alt*-CO). The low T_g of the *n*-alkyl substituted γ-polyketones was attributed to the reduction of dipole−dipole interactions between the ketones in the molecular chains.[1b,30] The uniquely high T_g of ester-containing γ-polyketones could be attributed to the stronger dipole−dipole interactions between molecular chains induced by the ester groups in addition to the ketone moieties. As for melting temperatures of poly(MA-*alt*-CO) and poly(CO-*alt*-(ethylene; MA)), no apparent signals were observed in DSC analyses.[31]

Thermogravimetry (TG) analyses (Figure 4) showed thermal decomposition starts at ca. 200 °C for both co- and terpolymers. In the case of the terpolymer, additional decomposition starts at 300 °C, which corresponds to the decomposition temperature of poly(ethylene-*alt*-CO).[1b]

5. Experimental Mechanistic Studies. In contrast to the catalysts described in Scheme 2, the Pd phosphine−sulfonate system could uniquely copolymerize methyl acrylate with carbon monoxide. This suggested that the Pd phosphine−sulfonate system allowed further insertion of monomers into five-membered chelate complex **3a** (Scheme 5),[11] while other Pd complexes resisted further reaction to **III** (Scheme 2).[7] In this section, the structure and the reactivity of these key five-membered chelate intermediates, [L−L]PdCH(CO_2Me)CH_2COMe (**3a**, **3c**−**e**), are compared.

First, we synthesized an analogous complex (**3c**) ligated by 1,2-bis(diphenylphosphino)ethane (DPPE) according to a modified procedure reported by van Leeuwen[7b] (see Experimental section) because complexes ligated by DPPE are some of the most frequently employed for the copolymerization of aliphatic olefins with CO.[1a,c,32] The copolymerization of MA with CO by **3c** did not proceed,[7b,33] but rather the formation of poly(methyl acrylate) was observed. Formation of the homopolymer could be initiated by adventitious radical species or homolytic cleavage of Pd−CH(CO_2Me)R bond.[34]

dx.doi.org/10.1021/ja2003268 |*J. Am. Chem. Soc.* 2011, 133, 6761–6779

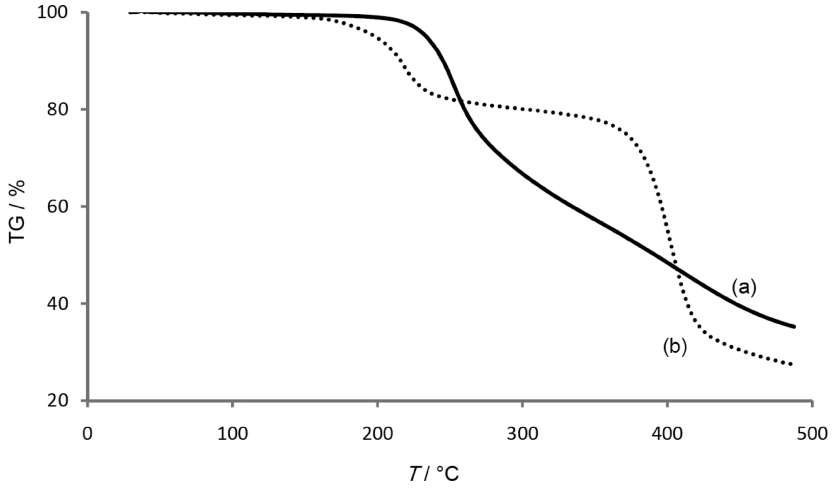

Figure 4. Thermolysis curves of (a) poly(MA-*alt*-CO) and (b) poly(CO-*alt*-(ethylene; MA)), entry 2 in Table 2.

Table 3. Comparison of the Experimental Pd−C and Pd−O Lengths (Å) of the Five-Membered Chelate Complexes

	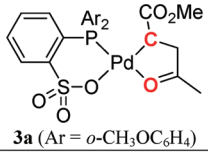 **3a** (Ar = *o*-$CH_3OC_6H_4$)	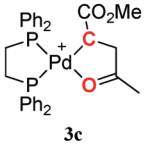 **3c**	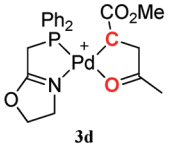 **3d**	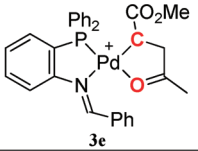 **3e**
Pd–C	2.042(6)	2.116(3)	2.046(4)	2.059(3)
Pd–O	2.137(4)	2.109(2)	2.112(2)	2.161(2)
X-ray source	ref. 11	Supporting Information	ref. 7h	ref. 7g

Next, the structures of the key intermediates were compared. Experimentally determined Pd−C and Pd−O bond lengths for a series of five-membered chelate intermediates are listed in Table 3. Although one might expect that the five-membered chelate in the active Pd phosphine−sulfonate complex **3a** would be more weakly[35] than the carbonyl oxygen of the inactive complexes (**3c**−**e**), its Pd−C (2.042(6) Å) and Pd−O (2.137(4) Å) distances are not significantly different than those in **3c**−**e**. The Pd−C bond length of **3a** is almost the same as those of **3d** and **3e**, while that of **3c** is slightly longer because of the strong *trans* influence of the phosphorus moiety located *trans* to the alkyl group. In this sense, the *trans* influence of a sulfonate group can be recognized as being as weak as an imine group.[36,37] In terms of Pd−O bond lengths, **3a** is within the range of **3d**−**e** as listed in Table 3.

Finally, the reactivities of these five-membered chelate complexes (**3a** and **3c**) with CO were investigated using a high pressure NMR apparatus.[38] Exposure of five-membered chelate complex **3a** to 6 MPa of CO at ambient temperature afforded a mixture of novel complexes along with the starting complex **3a** (Figure 5). In the ^{13}C NMR spectrum in CD_2Cl_2, new signals in the carbonyl region were observed at 181.3, 202.4, 205.3 ppm in addition to the signal of free CO at 183.8 ppm. Considering that the α-position of CO_2Me group shifted from 34.6 ppm to 63.7 ppm, the new complex observed was assigned to PdCOCH(CO_2Me)CH_2COCH_3 and the signal at 202.4 ppm (d, J = 16.1 Hz) was assigned to be that of the Pd−acyl carbonyl moiety located *cis* to the phosphine (C4 in Figure 5). Furthermore, a ketone functionality coordinated to the Pd center was not present, typically observed around 220−240 ppm.[7c] Instead, the $-CH_2COCH_3$ carbonyl signal was observed at 205.3 ppm, which indicates that the ketone carbonyl oxygen does not coordinate to the Pd center (C3).[7c] The fourth coordination site of Pd is occupied by the carbonyl oxygen of the ester group, which is observed at 181.3 ppm (br) (C5).[12f]

Therefore, the new signals were assigned as the complex [P−SO_3]Pd(CO)COCH(CO_2Me)CH_2COCH_3 (**5a**), formed by associative CO coordination (see Section 6), migratory insertion of CO, and *cis*/*trans* isomerization reaction (Scheme 6). Detailed assignments of the complex **5a** are shown in the Experimental section. Most of **5a** underwent decarbonylation after releasing the CO pressure to regenerate the five-membered complex **3a**.[39] This result suggests that the CO insertion to the complex **3a** is reversible even at ambient temperature.

In contrast, no new signals were detected in the carbonyl region after exposing the five-membered chelate complex **3c**, bearing DPPE ligand, to CO (6 MPa) (Scheme 6, see Supporting Information). This inert nature of **3c** toward CO insertion can be understood either by kinetic and/or thermodynamic reasoning, which will be discussed in Section 7.

Consequently, the comparison of the key five-membered chelate complexes bearing a phosphine−sulfonate (**3a**) and DPPE (**3c**) can be summarized as follows: (i) the structures of the complexes are similar, (ii) **3a** undergoes reversible insertion of CO to afford acylpalladium complex **5a**, (iii) the reaction of **3c** with CO does not afford an acylpalladium complex.

6. Mechanistic Studies by Theoretical Calculations. To study the detailed mechanism of the overall catalytic cycle, we conducted theoretical calculations. Our aim was to understand why the Pd phosphine−sulfonate system accomplished the

dx.doi.org/10.1021/ja2003268 |*J. Am. Chem. Soc.* 2011, 133, 6761–6779

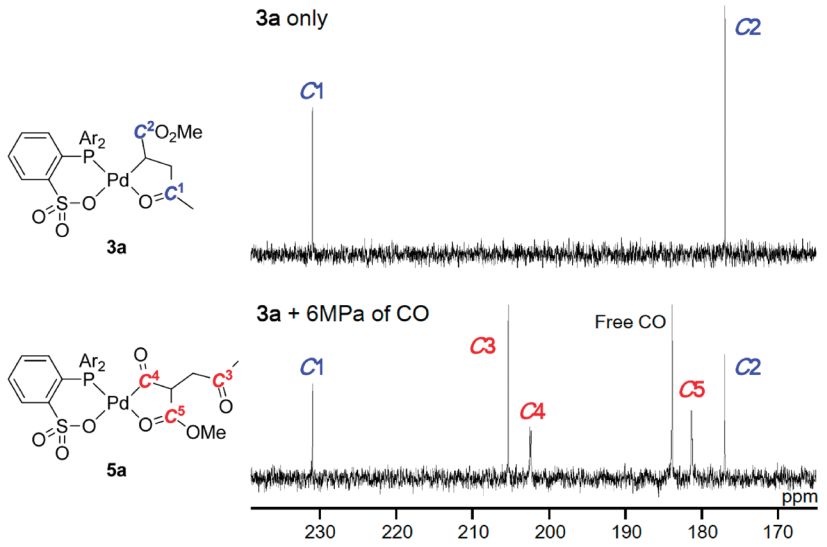

Figure 5. ^{13}C NMR (CD_2Cl_2) of complex **3a** (top) and **3a** + 6 MPa of CO using a high-pressure NMR tube (bottom). Representative signals are assigned to **3a** (blue) and **5a** (red). Ar = *o*-$CH_3OC_6H_4$, [P−O] = {*o*-((*o*-$MeOC_6H_4$)$_2$P)$C_6H_4SO_3$}.

Scheme 6. Reaction of Key Five-Membered Chelate Complexes 3a and 3c with 6 MPa of CO

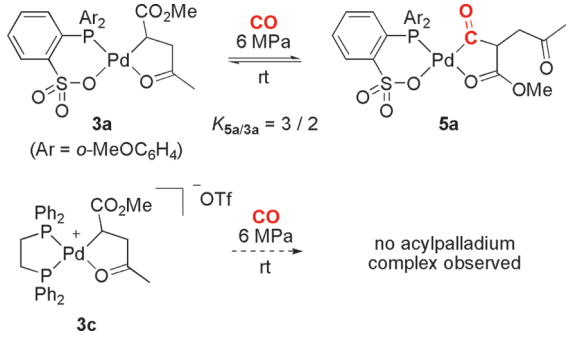

copolymerization of MA with CO while the Pd dppe complex, one of the most commonly used catalysts in the copolymerization of aliphatic olefins with CO,[1a,c] could not. In our theoretical studies, density functional theory method (B3LYP[40]/6-31G* and Lanl2dz[41]) was employed.[42] As ligands, diphenylphosphinobenzenesulfonate (deprotonated form of **1b**, see entry 2 in Table 1) and DPPE were used. Since both five-membered chelate complexes bearing phosphine−sulfonate (**3a**) and DPPE (**3c**) ligands were isolable and supposed to be stable intermediates in the catalytic cycles, we adopted these complexes as starting materials for the calculations.

Hereafter, the isomer having an X ligand (X = alkyl or acyl) and phosphorus atom in *cis* positions to each other will be described as "cis" for the united definition throughout the manuscript. In other words, an L ligand (L = carbonyl oxygen, CO, olefin) and phosphorus atom are *cis* to each other in the "trans" isomer (Figure 6). For example, $\mathbf{A}_{cis}$ is the *cis/trans* isomer of $\mathbf{A}_{trans}$. Additionally, we used an asterisk (*) to indicate the simplified chain replacement of the $-CH(CO_2CH_3)CH_2COCH_3$ group by a $-CH_3$ group. For instance, $^*\mathbf{D}_{cis}$ ([P−O]PdCOCH_3-(MA)) is the simplified structure of $\mathbf{D}_{cis}$ ([P−O]PdCOCH-$(CO_2CH_3)CH_2CH_3$(MA)). The simplified structures are used to scrutinize various possible pathways in some complexes while avoiding optimization of highly complicated structures having many possible conformations.

For all the stationary points, the relative energies with zero point energy correction (E+ZPC) and free energies (G, at 298.15 K and 1 atm) are listed in front of and behind the forward slash (/), respectively. The energies are expressed relative to the complexes $\mathbf{A}_{cis}$ and $\mathbf{A}_{PP}$ which are analogous to **3a** and **3c**, respectively. The optimized structures of $\mathbf{A}_{cis}$ and $\mathbf{A}_{PP}$ were in reasonable agreement with the X-ray crystal structures of **3a** and **3c** (see Supporting Information).[42]

The processes we studied include relative stabilities of *cis/trans* isomers of palladium phosphine−sulfonate complexes and their isomerization reactions (Section 6.1), CO coordination and insertion (Section 6.2), MA insertion (Section 6.3), and possible side reactions (Section 6.4). After the calculation of these essential reactions, we will discuss the overall catalytic cycle and compare the phosphine−sulfonate ligand with DPPE in Section 7.

6.1. Relative Stabilities of cis/trans Isomers and Their Isomerization Reactions. Due to the unsymmetric nature of the phosphine−sulfonate ligands, their square-planar palladium(II) complexes have both *cis/trans* isomers.[43] During our investigations on the stability of these isomers, as well as isomerization transition states in ethylene homopolymerization catalyzed by Pd phosphine−sulfonate complexes,[14] we found that the relative location of an alkyl group in all the intermediates was preferentially *cis* to the phosphine moiety (Figure 7). This preference can be attributed to the strong *trans* influence of the alkyl group and the phosphine moiety, which prefer not being *trans* to each other. This tendency was in agreement with the experimental fact that an alkyl group is positioned *cis* to the phosphine moiety in the X-ray structure of **3a**.[11] It is confirmed by DFT calculation that complex $\mathbf{A}_{cis}$, the analogue of **3a**, is more stable than its *cis/trans* isomer $\mathbf{A}_{trans}$ by 5.4/4.6 kcal/mol.

The above-mentioned preference is generally applicable to most of the intermediates in this article. However, carbonyl complexes were the only exceptions to this rule. The carbonyl complex $\mathbf{B}_{trans}$ is lower in energy than complex $\mathbf{B}_{cis}$ by 2.1/3.3 kcal/mol although the alkyl group in $\mathbf{B}_{trans}$ is *trans* to the

dx.doi.org/10.1021/ja2003268 |*J. Am. Chem. Soc.* 2011, 133, 6761–6779

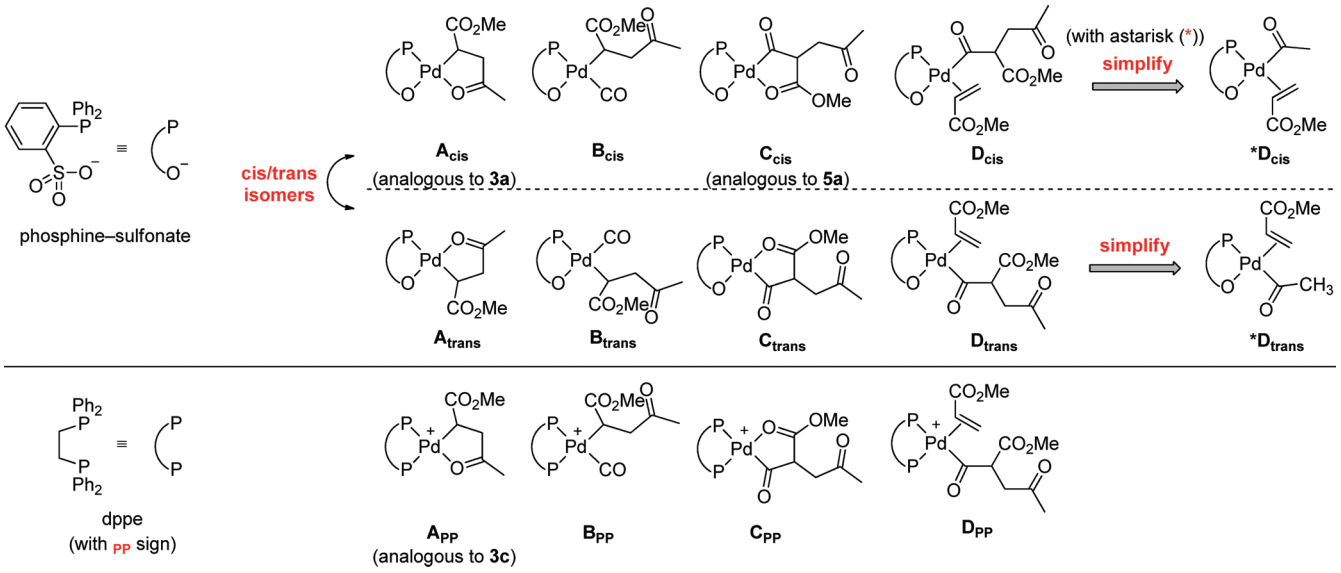

Figure 6. Definitions for the basic structures used in theoretical part.

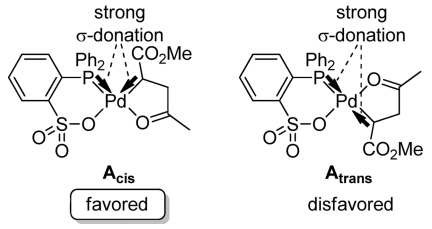

Figure 7. Standard *cis*/*trans* preference of Pd−alkyl complex $\mathbf{A}_{cis}$ and $\mathbf{A}_{trans}$.

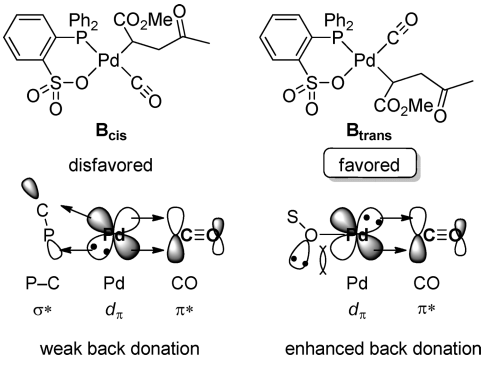

Figure 8. Conceptual pictures for the difference in back-donation between carbonyl complexes $\mathbf{B}_{cis}$ and $\mathbf{B}_{trans}$.

phosphine (Figure 8).[44] The reverse preference can be attributed to the strong *trans*-directing nature of carbon monoxide,[45] which avoids being *trans* to the phosphine. In addition, the back-donation from the filled d_π orbitals of the Pd center to the empty π^* orbitals of CO play a key role in the stabilization.[45b] In fact, the calculated distances between Pd and the carbon of CO (2.001 Å for $\mathbf{B}_{cis}$ vs 1.888 Å for $\mathbf{B}_{trans}$) and the bond lengths of CO (1.137 Å for $\mathbf{B}_{cis}$ vs 1.144 Å for $\mathbf{B}_{trans}$) suggested that the back-donation in $\mathbf{B}_{trans}$ is stronger than that in $\mathbf{B}_{cis}$ (Table 4). Thus, the back-donation to CO is enhanced when CO is *trans* to the sulfonate group ($\mathbf{B}_{trans}$) compared to its isomer ($\mathbf{B}_{cis}$). It is well-known that phosphines are efficient π-acceptors due to their P−C σ^* orbital overlapping with the d_π orbital of a metal center.[46] For this reason, the portion of π-back-donation from Pd to CO is decreased when CO is *trans* to the phosphine. On the other hand, the sulfonate group does not have an appropriate vacant orbital which can withdraw the electrons efficiently from a filled *d* orbital of a Pd center.[47] Thus, the sulfonate group can be considered as a weak π-acceptor. Furthermore, lone pairs on the oxygen atom of the sulfonate group can act as weak π-donors. The back-donation to CO should be further enhanced in order to avoid the repulsion between the filled d_π orbitals of Pd and filled nonbonding orbitals of the oxygen. These two characteristics (weak π-acceptor and weak π-donor) significantly contribute to the stronger back-donation from Pd to CO when it is located *trans* to the sulfonate (Figure 8).

The above-discussed difference in back-donation can also be seen in other intermediates (Figure 6). Aside from the carbonyl complexes, acylpalladium species and MA-coordinated complexes also exhibited stronger back-donation when these moieties are *trans* to the SO_3 group. Acyl groups in $\mathbf{C}_{cis}$, and $\mathbf{D}_{cis}$ exhibited a longer C═O bond than in $\mathbf{C}_{trans}$ and $\mathbf{D}_{trans}$, respectively. This is because π^* orbitals of C═O bond overlaps with filled *d* orbitals of Pd center. In addition, the distance between Pd and the olefin moiety of MA is shorter and C═C bond is longer in $\mathbf{D}_{trans}$ compared to those in $\mathbf{D}_{cis}$, suggesting that the back-donation from Pd to the electron deficient C═C is effective when the sulfonate is *trans* to MA. Although the acyl moiety and MA can accept the back-donation from the Pd center, the extent to which it occurs is weaker than CO. In fact, the stability of the series of $\mathbf{C}_{trans}$ and $\mathbf{D}_{trans}$ follows the standard *cis*/*trans* preference shown in Figure 7.

The back-donating ability of the cationic Pd dppe complexes are also compared and shown in Table 4. In the case of the Pd dppe complexes, CO, acyl moiety, and MA are always *trans* to the phosphorus atom. The bond lengths of a moiety in the Pd dppe complexes are more similar to the corresponding bond lengths in the isomer of the Pd phosphine−sulfonate complex where the moiety in question is *trans* to the phosphorus. For example, the Pd−C and C−O bond lengths of CO in $\mathbf{B}_{PP}$ (1.995 and 1.137 Å)

dx.doi.org/10.1021/ja2003268 |J. Am. Chem. Soc. 2011, 133, 6761–6779

Table 4. Calculated Bond Lengths (Å) for the Selected Intermediates Bearing a Phosphine−Sulfonate Ligand and a DPPE Ligand

		phosphine−sulfonate			DPPE
		trans to SO_3		*trans* to P	*trans* to P
Pd−CO	Pd−C	1.888 ($\mathbf{B}_{trans}$)	<	2.001 ($\mathbf{B}_{cis}$)	1.995 ($\mathbf{B}_{PP}$)
	C−O	1.144 ($\mathbf{B}_{trans}$)	>	1.137 ($\mathbf{B}_{cis}$)	1.137 ($\mathbf{B}_{PP}$)
Pd−C(O)Me	Pd−C	1.983 ($\mathbf{C}_{cis}$)	<	1.995 ($\mathbf{C}_{trans}$)	2.047 ($\mathbf{C}_{PP}$)
	C−O	1.209 ($\mathbf{C}_{cis}$)	>	1.199 ($\mathbf{C}_{trans}$)	1.201 ($\mathbf{C}_{PP}$)
	Pd−C	1.988 ($\mathbf{D}_{cis}$)	<	2.027 ($\mathbf{D}_{trans}$)	2.062 ($\mathbf{D}_{PP}$)
	C−O	1.204 ($\mathbf{D}_{cis}$)	>	1.196 ($\mathbf{D}_{trans}$)	1.201 ($\mathbf{D}_{PP}$)
Pd−MA	Pd−C	2.242−2.265 ($\mathbf{D}_{trans}$)	<	2.289−2.365 ($\mathbf{D}_{cis}$)	2.329−2.391 ($\mathbf{D}_{PP}$)
	C=C	1.382 ($\mathbf{D}_{trans}$)	>	1.379 ($\mathbf{D}_{cis}$)	1.374 ($\mathbf{D}_{PP}$)

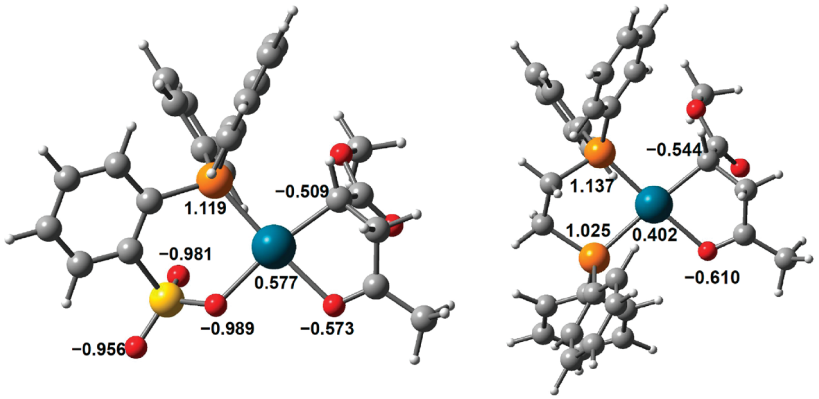

Figure 9. Charge distributions of $\mathbf{A}_{cis}$ and $\mathbf{A}_{PP}$ estimated by NBO population analyses (B3LYP/6-31G*, Lanl2dz).

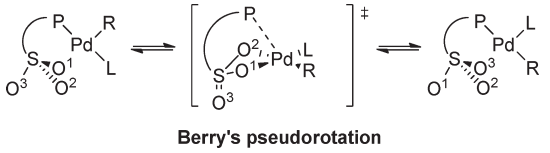

Figure 10. *Cis/trans* isomerization reaction via Berry's pseudorotation-like transition state.[14]

are quite close to those of $\mathbf{B}_{cis}$ (2.001 and 1.137 Å) rather than those of $\mathbf{B}_{trans}$ (1.888 and 1.144 Å).[48] Therefore, the back-donation in these complexes appears to be influenced primarily by the ligand located *trans* to CO. On the other hand, the contribution of the net charge of these complexes (i.e., neutral Pd phosphine−sulfonate and cationic Pd dppe) to the back-donating ability seems to be minor. In fact, NBO population analyses[49] showed that the negative charge is mainly located on the oxygen atoms of the sulfonate group for the Pd phosphine−sulfonate complexes, and the charge on Pd is almost the same as that for the cationic Pd dppe complex (For the case of $\mathbf{A}_{cis}$ and $\mathbf{A}_{PP}$, see Figure 9). Thus, the ability of back-donation depends not on the net charge of the complexes but mainly on the stereoelectronic effect of the *trans* ligands and the palladium center.

Previously, we proposed that *cis/trans* isomerization of Pd phosphine−sulfonate proceeds via so-called Berry's pseudorotation of pentacoordinated complexes involving the associative exchange of the oxygen atoms in the sulfonate group (Figure 10).[14] One of the most unique characteristics of Pd phosphine−sulfonate complexes is that the pentacoordinate TS is lower in energy than that of the corresponding simple rotation TS. We also investigated transition states of *cis/trans* isomerization required for the copolymerization of MA with CO and showed that **TS**($\mathbf{C}_{cis}$−$\mathbf{C}_{trans}$) and **TS**($\mathbf{D}_{cis}$−$\mathbf{D}_{trans}$) represent pentacoordinated Berry's pseudorotation transition states, which need only 7.2/7.0 (from $\mathbf{C}_{trans}$), and 7.3/8.0 (from $\mathbf{D}_{trans}$) kcal/mol, respectively (in Scheme 7 and Scheme 10). Between $\mathbf{A}_{cis}$ and $\mathbf{A}_{trans}$ and between $\mathbf{B}_{cis}$ and $\mathbf{B}_{trans}$, pentacoordinate structures **Amed** and **Bmed** were found as intermediates instead of TS (Scheme 7).[50]

6.2. CO Coordination and Insertion. The alternating copolymerization is initiated by CO coordination to five-membered chelate complex $\mathbf{A}_{cis}$ (Scheme 7). For the 16e d^8 square planar Pd complex, the associative ligand substitution is widely accepted, particularly with the strong π-acceptor CO.[51] As expected, chelate opening by CO can take place via trigonal-bipyramidal transition states either from $\mathbf{A}_{cis}$ or $\mathbf{A}_{trans}$ with barriers of 5.0/15.2 and 9.3/18.4 kcal/mol from $\mathbf{A}_{cis}$, respectively.[52] Through **TS**($\mathbf{A}_{cis}$−$\mathbf{B}_{cis}$) and **TS**($\mathbf{A}_{trans}$−$\mathbf{B}_{trans}$), the CO molecule moves to the equatorial plane and the chelating carbonyl group moves away from the equatorial plane.[44]

The transition states for the subsequent CO insertion into the Pd−C bond were successfully located both from $\mathbf{B}_{cis}$ and $\mathbf{B}_{trans}$. **TS**($\mathbf{B}_{trans}$−$\mathbf{C}_{cis}$) is lower in energy than **TS**($\mathbf{B}_{cis}$−$\mathbf{C}_{trans}$) by 11.4/10.8 kcal/mol mainly because the alkyl group in $\mathbf{B}_{trans}$ is more activated for the migratory insertion by the stronger *trans* effect of the phosphine moiety than the sulfonate oxgen.[14,16,43]

dx.doi.org/10.1021/ja2003268 |*J. Am. Chem. Soc.* 2011, 133, 6761–6779

Scheme 7. CO Coordination and Insertion to Five-Membered Chelate Complex Bearing Phosphine−Sulfonate Ligand (E+ZPE/G, kcal/mol). The red arrow exhibits the most preferable pathway

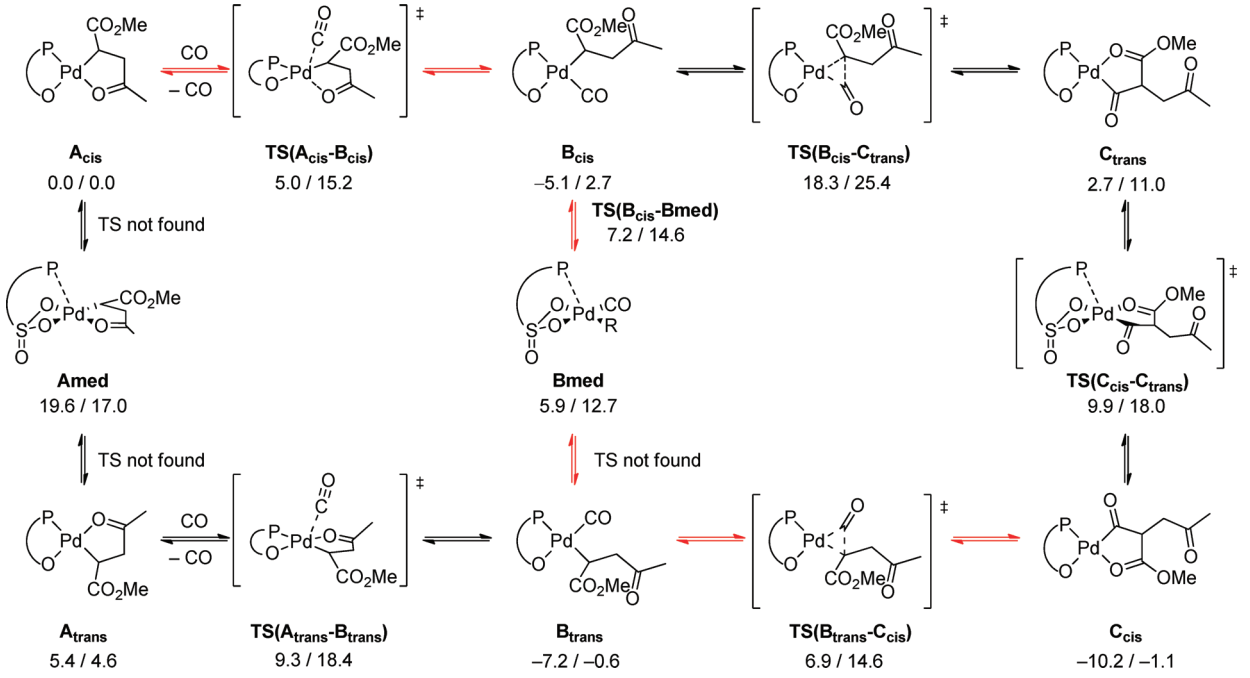

Scheme 8. CO Coordination and Insertion to Five-Membered Chelate Complex Bearing DPPE Ligand (E+ZPE/G, kcal/mol)

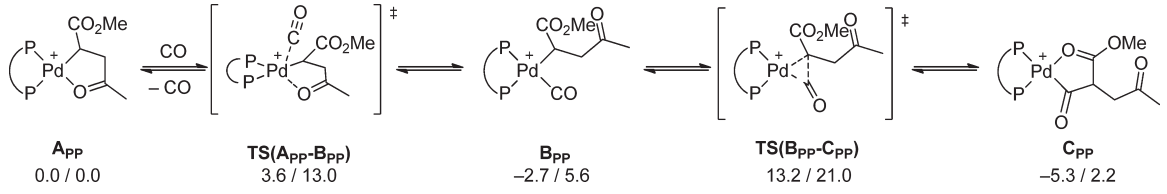

In fact, the Pd−C (alkyl chain) bond length in $\mathbf{B}_{trans}$ (2.152 Å) is longer than that in $\mathbf{B}_{cis}$ (2.109 Å). Accordingly, CO insertion takes place from $\mathbf{B}_{trans}$ after CO coordination to the five-membered chelate complex $\mathbf{A}_{cis}$, accompanied by *cis/trans* isomerization via **Bmed**.[53] After CO insertion, the internal ester carbonyl oxygen coordinates to the Pd center to afford a five-membered chelate complex $\mathbf{C}_{cis}$ as observed in experiment (**5a**, Figure 5).[54]

For comparison, we calculated the reaction pathways of CO coordination and insertion toward $\mathbf{A}_{PP}$ bearing a DPPE ligand (Scheme 8). Associative CO coordination via $\mathbf{TS}(\mathbf{A}_{PP}-\mathbf{B}_{PP})$ requires a barrier of 3.6/13.0 kcal/mol from $\mathbf{A}_{PP}$, which is similar to the case of the Pd phosphine−sulfonate complex ($\mathbf{TS}(\mathbf{A}_{cis}-\mathbf{B}_{cis})$, 5.0/15.2 kcal/mol). This result indicates that a *high barrier for CO coordination is not the reason why Pd dppe complexes cannot copolymerize MA and CO* (Scheme 2).[7b] Subsequently, CO insertion can take place via $\mathbf{TS}(\mathbf{B}_{PP}\text{-}\mathbf{C}_{PP})$ with a barrier of 13.2/21.0 kcal/mol.[55] The interpretation of these calculations and experiments in Section 5 will be discussed in Section 7.

6.3. MA Insertion. After insertion of CO into five-membered chelate complexes (Section 6.2), MA should react with the acylpalladium species to complete the catalytic cycle. Since it was difficult to calculate all conformations of the highly complex intermediates, we first studied MA insertion into a simple Pd−acetyl (PdCOMe) bond as a model instead of the Pd−CH-$(CO_2CH_3)CH_2COCH_3$ group (i.e., we first used $^*\mathbf{D}_{cis}$ and $^*\mathbf{D}_{trans}$ instead of $\mathbf{D}_{cis}$ and $\mathbf{D}_{trans}$). While the MA insertion into Pd−alkyl bonds has been widely studied by theoretical calculations,[12f,56,57] this is the first theoretical study dealing with MA insertion into a Pd−acetyl bond to the best of our knowledge.[1h]

From *cis/trans* isomers of PdCOMe(MA) complex $^*\mathbf{D}_{cis}$ and $^*\mathbf{D}_{trans}$, two types of MA insertion pathways, i.e., 2,1- and 1,2-insertion, could proceed (Scheme 9). Both 2,1- and 1,2-insertion transition states from $^*\mathbf{D}_{cis}$ and $^*\mathbf{D}_{trans}$ were successfully located. It was found that 2,1-insertion predominates over 1,2-insertion (i.e., $\mathbf{TS}(^*\mathbf{D}_{trans}-\mathbf{A}_{cis})$ and $\mathbf{TS}(^*\mathbf{D}_{cis}-\mathbf{A}_{trans})$ lower in energy than $\mathbf{TS}(^*\mathbf{D}_{trans}-\mathbf{E}_{cis})$ and $\mathbf{TS}(^*\mathbf{D}_{cis}-\mathbf{E}_{trans})$, respectively). This is consistent with the experimental result that **3a** was obtained as the sole product when MA was added to the solution of **4a** (Scheme 3). The strong preference toward 2,1-insertion results in highly regiocontrolled architecture of the copolymer, as confirmed in Section 2.[58] The preference toward 2,1-insertion could be attributed to three

dx.doi.org/10.1021/ja2003268 |*J. Am. Chem. Soc.* 2011, 133, 6761–6779

Scheme 9. MA Insertion into the Pd−Acetyl Bond by Pd Phosphine−Sulfonate Complexes (E+ZPE/G, kcal/mol)[a]

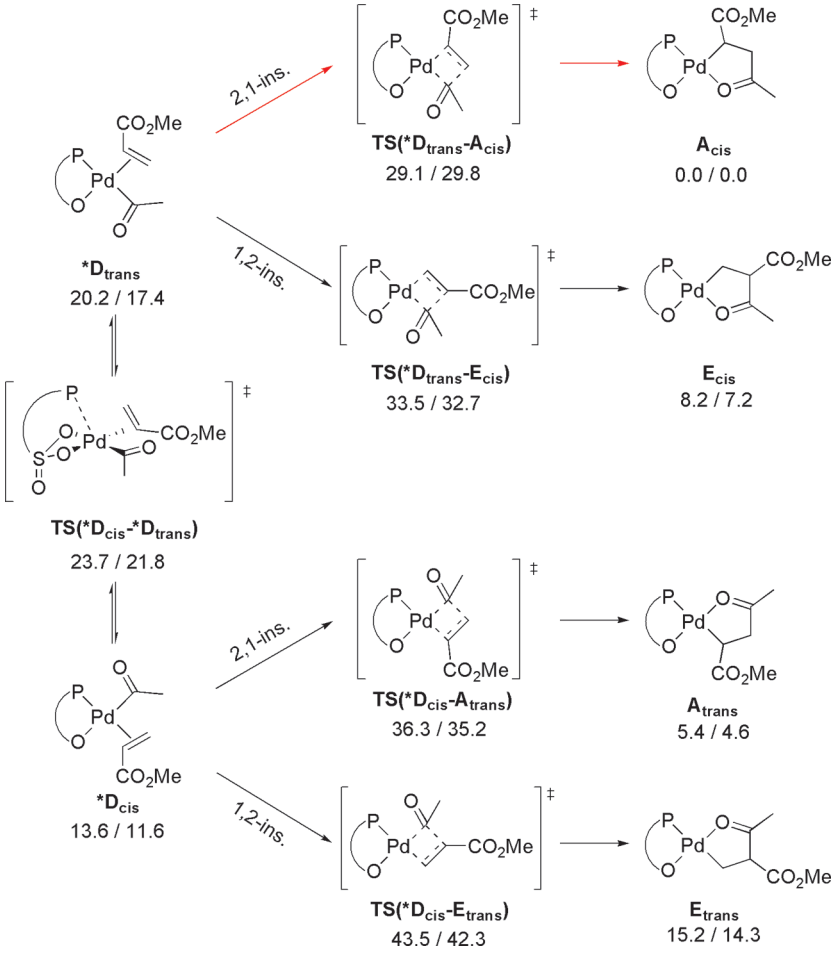

[a] The long alkyl chain (Pd−COCH(CO_2Me)CH_2COCH_3) was simplified to Pd−$COCH_3$. The red arrow shows the lowest energy pathway.

factors: (i) steric repulsion between the migrating acetyl group and the methoxycarbonyl group should disfavor 1,2-insertion,[56a] (ii) electron-withdrawing nature of the methoxycarbonyl group makes a difference in LUMO orbital (C═C, $2p_z$) coefficients to some extent, which strengthen the 2,1-insertion preference,[56a] and (iii) the energies required for the distortion of MA through 2,1-insertion from MA-coordinated species are smaller compared to those of 1,2-insertion.[56b,57a] In fact, a smaller distortion energy for the 2,1-insertion was also found in the case of MA inserting into the Pd−acetyl bond (see Supporting Information). In contrast, *t*-butyl acrylate underwent both 2,1- and 1,2-insertion (Section 2) because the steric repulsion between the ligand and the *t*-butoxycarbonyl group was large enough to compete with the factors above (i−iii).

It was also found that the insertion from $^*\mathbf{D}_{\mathbf{trans}}$ is more favorable than that from $^*\mathbf{D}_{\mathbf{cis}}$ (i.e., $\mathbf{TS}(^*\mathbf{D}_{\mathbf{trans}}-\mathbf{A}_{\mathbf{cis}})$ and $\mathbf{TS}(^*\mathbf{D}_{\mathbf{trans}}-\mathbf{E}_{\mathbf{cis}})$ are lower in energy than $\mathbf{TS}(^*\mathbf{D}_{\mathbf{cis}}-\mathbf{A}_{\mathbf{trans}})$ and $\mathbf{TS}(^*\mathbf{D}_{\mathbf{cis}}-\mathbf{E}_{\mathbf{trans}})$, respectively). The preference is due to the stronger *trans* effect of the phosphine moiety than the sulfonate group; the acetyl group in $^*\mathbf{D}_{\mathbf{trans}}$ is more activated toward migratory insertion.[14,16,43] In fact, the Pd−C bond length in $^*\mathbf{D}_{\mathbf{trans}}$ (2.028 Å) is longer than that in $^*\mathbf{D}_{\mathbf{cis}}$ (1.993 Å). This tendency suggests that the MA insertion into the Pd−acyl bond can be recognized as acyl anion migration to MA. Moreover, it was found that the order of the relative energy of these transition states generally reflects the order of the stability of the products ($\mathbf{E}_{\mathbf{trans}}$ > $\mathbf{E}_{\mathbf{cis}}$ > $\mathbf{A}_{\mathbf{trans}}$ > $\mathbf{A}_{\mathbf{cis}}$ (the most stable)).

According to the results obtained in the simplified model, 2,1-insertion of MA from **D** is suggested to be the most preferable pathway. Thus, we calculated the route $\mathbf{D}_{\mathbf{cis}}\rightarrow\mathbf{TS}(\mathbf{D}_{\mathbf{cis}}-\mathbf{D}_{\mathbf{trans}})\rightarrow\mathbf{D}_{\mathbf{trans}}\rightarrow\mathbf{TS}(\mathbf{D}_{\mathbf{trans}}-\mathbf{A}_{\mathbf{cis}}\mathbf{next})\rightarrow\mathbf{A}_{\mathbf{cis}}\mathbf{next}$ using full-size PdCOCH(CO_2Me)CH_2COCH_3 complexes (Scheme 10). It should be noted that the transition state for MA coordination to complexes $\mathbf{C}_{\mathbf{cis}}$ or $\mathbf{C}_{\mathbf{trans}}$ could not be located possibly because of nearly flat potential energy surface.[59] We assume that the barrier of the coordination is negligible compared to the subsequent insertion barrier.[12f,14,57] Since the insertion of MA, $\mathbf{TS}(\mathbf{D}_{\mathbf{trans}}-\mathbf{A}_{\mathbf{cis}}\mathbf{next})$, needs 3.9/27.2 kcal/mol from complex $\mathbf{A}_{\mathbf{cis}}$, this acrylate insertion has the highest barrier through the catalytic cycle from $\mathbf{A}_{\mathbf{cis}}$ to $\mathbf{A}_{\mathbf{cis}}\mathbf{next}$, and makes it the rate-determining step.

Similarly, 2,1-insertion of MA into a Pd−acyl bond of Pd dppe complexes was also examined (Scheme 11). By using the full-size PdCOCH(CO_2Me)CH_2COMe complex, 2,1-insertion of MA could proceed with a barrier of 11.3/33.6 kcal/mol from $\mathbf{A}_{\mathbf{PP}}$ via $\mathbf{D}_{\mathbf{PP}}\rightarrow\mathbf{TS}(\mathbf{D}_{\mathbf{PP}}\text{-}\mathbf{A}_{\mathbf{PP}}\mathbf{next})\rightarrow\mathbf{A}_{\mathbf{PP}}\mathbf{next}$. The MA insertion is, again, a rate-determining step because this has the highest energy in the catalytic cycle from $\mathbf{A}_{\mathbf{PP}}$ to $\mathbf{A}_{\mathbf{PP}}\mathbf{next}$. In addition, the MA insertion TS for the Pd dppe complex is less favorable than that for the Pd phosphine−sulfonate complexes by 7.4/6.4 kcal/mol.

dx.doi.org/10.1021/ja2003268 |*J. Am. Chem. Soc.* 2011, 133, 6761–6779

Scheme 10. MA Insertion into Pd−Acyl Bond of Pd Phosphine−Sulfonate Complexes (E+ZPE/G, kcal/mol)[a]

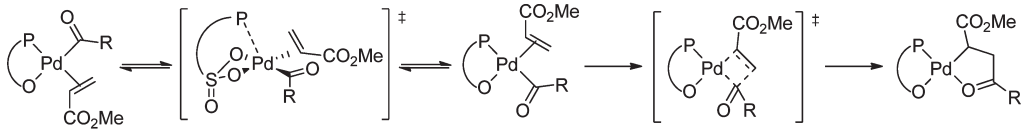

[a] R = $CH(CO_2Me)CH_2COMe$.

Scheme 11. MA Insertion into Pd−Acyl Bond of Pd dppe Complexes (E+ZPE/G, kcal/mol)[a]

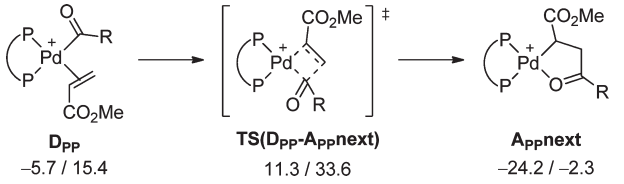

[a] R = $CH(CO_2Me)CH_2COMe$.

6.4. Possible Side Reactions.[34] In the presence of CO, double olefin insertion is generally disfavored because coordination of CO and subsequent insertion after olefin insertion is much faster than the second olefin insertion.[1,7c,52,60,61] In our experimental studies, the reaction of MA with CO catalyzed by the Pd phosphine−sulfonate complexes afforded completely alternating copolymers without any signal corresponding to double insertion of MA by NMR analysis, as discussed in Section 2. However, the Pd phosphine−sulfonate catalyst is a potent catalyst capable of producing nonalternating ethylene/CO copolymers with excess ethylene contents by the coordination−insertion mechanism.[15,16] Recently, Caporaso and Mecking experimentally and theoretically demonstrated that double (or more) insertion of MA can take place in the absence of CO.[12d,f] Thus, it is important to understand why double MA insertion does not occur when Pd phosphine−sulfonate complexes are employed in the presence of CO.

From complex $\mathbf{A_{cis}}$ (after insertion of one MA), another MA can coordinate *cis* to the phosphine ($\mathbf{F_{trans}}$), which is endothermic/endergonic by 15.7/27.2 kcal/mol. Migratory insertion of the alkyl groups *trans* to the phosphine ($\mathbf{TS(F_{trans}-G_{cis})}$) requires an overall barrier of 25.5/38.3 kcal/mol (Scheme 12). This is consistent with the overall barrier for multiple coordination−insertion of MA reported by Caporaso and Mecking (ca. 25 kcal/mol in ΔE).[12f] This route is thought to be the most probable pathway according to their detailed calculations. The barrier relative to $\mathbf{A_{cis}}$ is higher in energy than that of the alternating copolymerization cycle which requires an overall barrier of 3.9/27.2 kcal/mol ($\mathbf{TS(D_{trans}-A_{cis}next)}$, Scheme 10). Therefore, MA double insertion did not occur because it is kinetically disfavored in the presence of CO. Concerning the nonalternating copolymerization of ethylene with CO, it was reported that ethylene coordination into the five-membered chelate complex [P−O]$PdCH_2CH_2COEt$ is exothermic (−7.5 kcal/mol in ΔH) and successive insertion can take place with a barrier of 25.0 kcal/mol (in ΔH) from the chelate complex.[16a] Thus, difference in the ability of double insertion in the presence of CO can be attributed to the lower binding affinity of the electron-deficient MA compared to that of ethylene.[28,56]

7. Discussion on the Mechanism: Why Phosphine−Sulfonate? According to the discussion above, the most probable pathway for the full catalytic cycle of MA/CO copolymerization by the Pd phosphine−sulfonate complex is summarized in Figure 11 (bold line).[62] First, CO coordinates to the five-membered chelate complex $\mathbf{A_{cis}}$ to form carbonyl complex $\mathbf{B_{cis}}$ and, after *cis*/*trans* isomerization, CO insertion takes place to generate $\mathbf{C_{cis}}$ which was observed in high pressure NMR as **5a** in Section 5. After the coordination of MA to $\mathbf{C_{cis}}$ and *cis*/*trans* isomerization, exclusive 2,1-insertion takes place from complex $\mathbf{D_{trans}}$ to regenerate the five-membered chelate complex $\mathbf{A_{cis}next}$. The rate-determining step of the catalytic cycle is the MA insertion step via $\mathbf{TS(D_{trans}-A_{cis}next)}$, which is 27.2 kcal/mol higher in energy than $\mathbf{A_{cis}}$. The double insertion of either MA or CO[61] was energetically unfavorable.

The dotted line in Figure 11 shows the catalytic cycle for the Pd dppe system. Similarly, CO coordination and insertion takes place from the five-membered chelate complex $\mathbf{A_{PP}}$ to afford acylpalladium complex $\mathbf{C_{PP}}$. Then, MA coordination and insertion through the highest barrier via $\mathbf{TS(D_{PP}-A_{PP}next)}$ (33.6 kcal/mol from $\mathbf{A_{PP}}$) complete the catalytic cycle.

With the full catalytic cycle in hand (Figure 11), the experimental results were interpreted in detail. The obvious difference between the phosphine−sulfonate system and dppe system is recognized in the difference of the highest barriers, $\mathbf{TS(D_{trans}-A_{cis}next)}$ vs $\mathbf{TS(D_{PP}-A_{PP}next)}$. This is consistent with the experimental fact that the Pd phosphine−sulfonate complex **3a** copolymerized MA with CO while the Pd dppe complex **3c** did not.

Concerning the high-pressure NMR experiments in Section 5, CO insertion observed from the Pd phosphine−sulfonate complex **3a** could be attributed to the fact that the barriers for CO coordination ($\mathbf{TS(A_{cis}-B_{cis})}$) and insertion ($\mathbf{TS(B_{trans}-C_{cis})}$) are reasonably low to be overcome at ambient temperature and that the resulting acylpalladium complexes are stable enough to be observed.[54] In contrast, when Pd dppe complex **3c** was exposed to 6 MPa of CO at ambient temperature,[38] no new signals were detected. This result could be explained as follows (i) acylpalladium complexes were not detected because the barrier for CO insertion ($\mathbf{TS(B_{PP}-C_{PP})}$) cannot be overcome at ambient temperature (kinetic argument), *and* (ii) carbonyl complexes were also not observed since $\mathbf{B_{PP}}$ is less stable than $\mathbf{A_{PP}}$ by 5.6 kcal/mol (which corresponds to $K < 0.1$), although the barrier for the coordination, $\mathbf{TS(A_{PP}-B_{PP})}$, is easy to overcome (thermodynamic argument).

Before our first report on the copolymerization of MA with CO by the Pd phosphine−sulfonate system,[11] several attempts on this copolymerization had been reported (Scheme 2). It was proposed that the one possible reason for the inert nature of the five-membered chelate complexes[1h] is the lower nucleophilicity of the carbon α to the Pd center as a result of the electron-withdrawing group.[7b,8d] In fact, the CO insertion from

dx.doi.org/10.1021/ja2003268 |*J. Am. Chem. Soc.* 2011, 133, 6761–6779

Scheme 12. Double MA Insertion into Pd−Alkyl Bond of Pd Phosphine−Sulfonate Complexes (E+ZPE/G, kcal/mol)

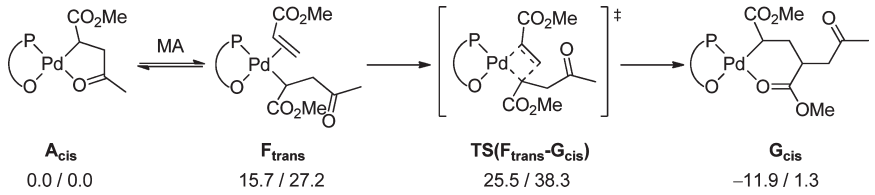

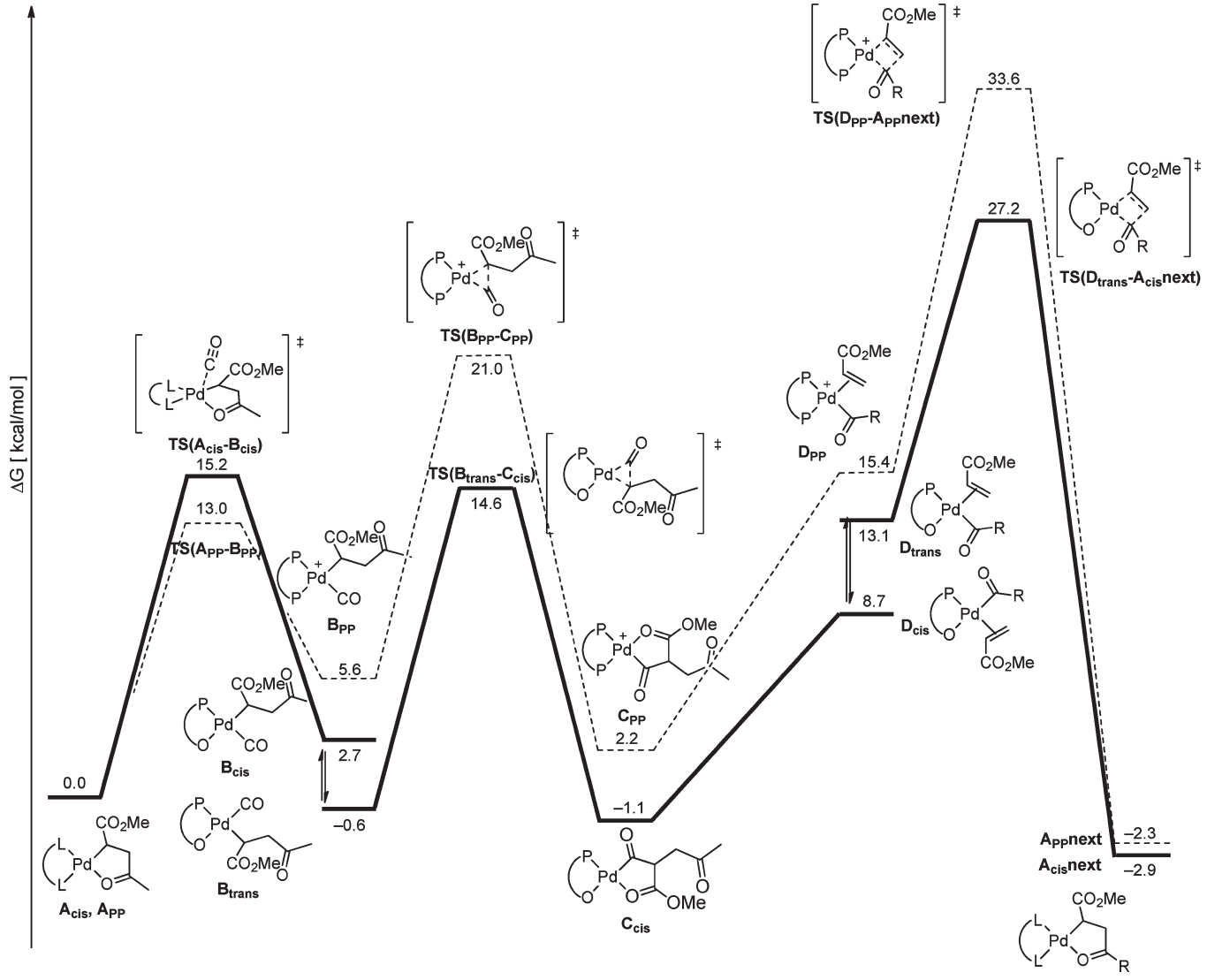

Figure 11. Comparison of the energy profiles for the copolymerization of MA with CO catalyzed by Pd phospine−sulfonate complex (**Bold black**) and Pd dppe complex (dotted line). The Gibbs free energies (in kcal/mol) relative to $\mathbf{A_{cis}}$ or $\mathbf{A_{PP}}$ are given. R = $CH(CO_2Me)CH_2COMe$.[62]

[P−O]Pd(CO)$CH_2CH_2COCH_3$ (without $-CO_2Me$ group) requires only a barrier of 11.5 kcal/mol,[16a] while the CO insertion from $\mathbf{B_{trans}}$ requires a barrier of 15.6 kcal/mol (Figure 11). Thus, it is the case that an electron-withdrawing group on the α-carbon slows down the CO insertion rate and, thus, the acylpalladium species would not be observed at ambient temperature (Scheme 6). However, Figure 11 suggests that coordination and insertion of CO are possible if higher temperature is provided because of their moderate barriers (13.0 and 21.0 kcal/mol, respectively).[38] Instead, the subsequent coordination−insertion of MA requires a rather high barrier (via **TS($\mathbf{D_{PP}}$−$\mathbf{A_{PP}}$next)**, 33.6 kcal/mol from $\mathbf{A_{PP}}$), which would be the main obstacle for the copolymerization by the Pd dppe complex.

All of these observations raise an important question: why do the Pd phosphine−sulfonate complexes make the copolymerization possible? The relative energy of the rate-determining MA insertion is lower for this Pd phosphine−sulfonate system compared to that of the Pd dppe system (Figure 11). This could

dx.doi.org/10.1021/ja2003268 |*J. Am. Chem. Soc.* 2011, 133, 6761–6779

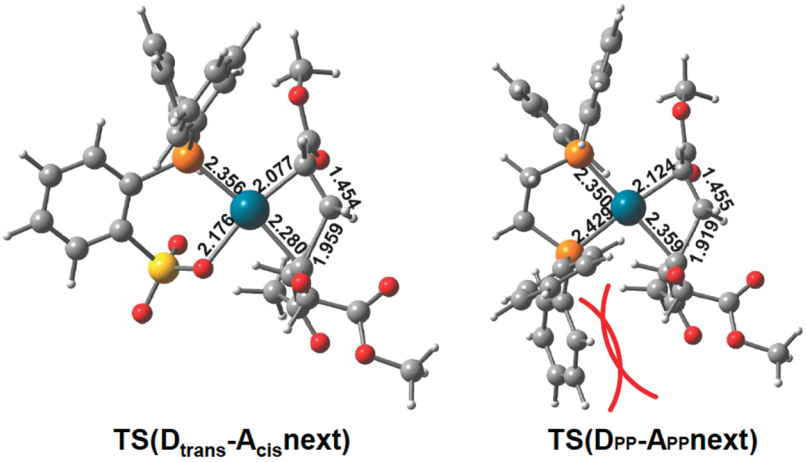

Figure 12. Calculated structures of the rate-determining step: **TS(D_{trans}−A_{cis}next)** and **TS(D_{PP}−A_{PP}next)**.

be attributed to the steric repulsion between the bulky Ph groups on the phosphorus atoms of DPPE and the polymer chain in the transition state (Figure 12). In contrast, the sulfonate group is not bulky and, therefore, **TS(D_{trans}−A_{cis}next)** is sufficiently low in energy to be overcome.

The second reason for the lower-energy transition state of MA insertion when using the Pd phosphine−sulfonate system is electronic in nature. Because of the early nature of the MA insertion TS,[63] they should have similar structures to precursor complexes, $\mathbf{D}_{trans}$ and $\mathbf{D}_{PP}$. It was found by comparing the structure of $\mathbf{D}_{trans}$ and $\mathbf{D}_{PP}$ that the C=C bond of MA in $\mathbf{D}_{trans}$ is longer than in $\mathbf{D}_{PP}$ and also that the Pd−olefin distance is shorter in $\mathbf{D}_{trans}$ than $\mathbf{D}_{PP}$ (Table 4). The results indicate that the back-donation from Pd to the electron-deficient olefin moiety is more efficient in the Pd phosphine−sulfonate than in the Pd dppe. The stronger back-donation should contribute to the higher stability of $\mathbf{D}_{trans}$. The lower-energy **TS(D_{trans}−Anext)** can also be explained by the fact that the olefin moiety of MA is more activated by the stronger back-donation from Pd to π^*(C=C) of MA. Thus, the longer carbon−carbon bond length of the bound MA facilitates the conversion from sp^2 to sp^3 hybridization.

It should be noted that most of the intermediates in Figure 11 (except $\mathbf{A}_{cis}$) and transition states are lower in energy in the Pd phosphine−sulfonate system compared to those of the Pd dppe system. This is because the back-donation from Pd to CO, acyl groups, or MA in these intermediates is facilitated when the sulfonate moiety is located *trans* to these substituents. As we discussed in Section 6.1, the main contribution to this stronger back-donation is not the neutral character of these complexes, but rather a stereoelectronic effect of the sulfonate moiety. In other words, the SO_3 group does not withdraw the π-electrons from Pd but, instead, repulsion between lone pairs on the ligated oxygen and π-electrons of Pd facilitates the back-donation to CO, acyl group or MA, which is located *trans* to the sulfonate moiety. Only the intermediate $\mathbf{A}_{cis}$ cannot be stabilized by back-donation because of a lack of appropriate low-lying vacant orbitals of the alkyl group.

CONCLUSIONS

In this article we provided the full details for the copolymerization of acrylates with CO catalyzed by a Pd phosphine−sulfonate system. The regiochemistry of poly(methyl acrylate-*alt*-CO) was excellently controlled, even though its methine carbons were gradually epimerizing in the presence of MeOH. Terpolymers of MA, ethylene, and CO were also synthesized by the same catalyst and its ester content could be controlled by changing the ethylene pressure. The incorporation of the ester group into γ-polyketones resulted in an increase in glass-transition temperature.

The mechanism for the alternating copolymerization of MA with CO catalyzed by the Pd phosphine−sulfonate complexes is summarized in Figure 13. Reversible CO insertion to isolated five-membered chelate complex **3a** was observed by high-pressure NMR study. Next, exclusive 2,1-insertion of MA takes place to regenerate the five-membered chelate complex, resulting in the regiocontrolled architectures of the copolymer. Subsequent MA insertion is not preferable because of its high energy barrier and the weak binding ability of MA. DFT calculation showed that the rate-determining step is MA insertion into the Pd-acyl bond activated by the *trans* phosphine ligand. It was found by comparison with the conventional Pd dppe system that the barrier of MA insertion for the Pd phosphine−sulfonate system was decreased for the following two reasons: (i) the sulfonate group is less hindered than the phosphine group and (ii) a coordinating MA is more activated due to the stronger back-donation from a Pd center. The enhanced back-donation can be mainly attributed to the weak π-acceptor character of the sulfonate group and the electronic repulsion between lone pairs of the sulfonate oxygens and π-electrons of a Pd center. Throughout this study, the role of this simple and elegantly designed unsymmetrical ligand has been revealed by an understanding of its molecular orbitals and their effect on the Pd center.[64,65] We believe that these detailed studies will allow the further design of novel catalysts.

EXPERIMENTAL SECTION

General Methods. All manipulations were carried out using standard glovebox or Schlenk techniques under argon purified by passing through a hot column packed with BASF catalyst R3−11. NMR spectra were recorded on JEOL JNM-ECP500 (^{1}H: 500 MHz, ^{2}H: 77 MHz, ^{13}C: 126 MHz, ^{31}P: 202 MHz with digital resolution of 0.239, 0.141 Hz, 0.960, 4.33 Hz, respectively) or JEOL JNM-ECS400 (^{1}H: 400 MHz, ^{13}C: 101 MHz, ^{31}P: 162 MHz with digital resolution of

dx.doi.org/10.1021/ja2003268 |*J. Am. Chem. Soc.* 2011, 133, 6761–6779

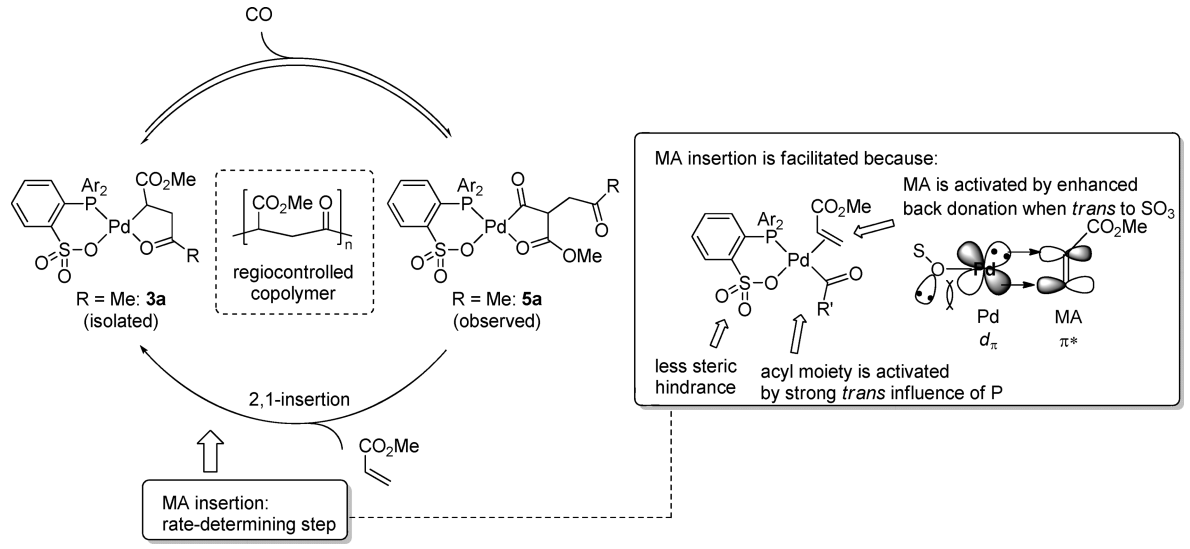

Figure 13. Summary of the mechanism of the copolymerization of methyl acrylate with CO catalyzed by a Pd phosphine−sulfonate complex and the role of sulfonate moiety.

0.09125, 0.767, 3.46 Hz, respectively) NMR spectrometers. Size exclusion chromatography (SEC) analyses were carried out at 40 °C with a GL Sciences instrument (model PU 610 high-performance-liquid-chromatography pump, CO 631A liquid chromatography column oven, and RI 713 refractive-index detector) equipped with two columns (Shodex KF-804 L) by eluting the columns with chloroform at 1 mL/min. Molecular weights were determined using narrow polystyrene standards. Fast atom bombardment mass spectrometry (FAB-MS) was carried out on a JEOL JMS-700 spectrometer using PEG calibration and NBA matrix solvent. Differential scanning calorimetry (DSC) analysis was performed on a SII EXTAR DSC-7020, with a heating rate of 10 K/min from −50 to 160 °C. Thermogravimetric analysis (TGA) of the polymers was measured on a SII EXTAR6000 TG/DTA-6200, with heating rate of 10 K/min form 30 to 500 °C. X-ray crystallographic analyses were performed on a Rigaku Mercury CCD diffractometer.

Materials Information. Anhydrous solvents (dichloromethane, diethyl ether, hexane, and tetrahydrofuran) were purchased from Kanto Chemical Co. Inc. and purified by the method of Pangborn et al.[66] Carbon monoxide (>99.95 vol%) was obtained from Takachiho Chemical Industrial Co. Ethylene (>99.9%) was purchased from Takachiho Chemical Industrial Co., Ltd., dried, and deoxygenated by passing through columns. Methyl acrylate and *t*-butyl acrylate were purchased from Kanto Chemical Co. Inc. and purified by vacuum-transfer over CaH_2 and stored under dark, argon, at −20 °C. 1,1,1,3,3,3-hexafluoro-2-propanol (Kanto) and methan-(ol-*d*) (Aldrich, 99 atom %-D) were purchased and used as received.

The following compounds were prepared according to literature procedures: $Pd(dba)_2$,[17] $Pd_2(dba)_3 \cdot CHCl_3$,[17] 2-{di(2-methoxyphenyl)phosphino}benzenesulfonic acid (**1a**),[15a] 2-(diphenylphosphino)-benzenesulfonic acid (**1b**),[13b] [{*o*-(*o*-$MeOC_6H_4)_2P$}$C_6H_4SO_3$]PdMe(2,6-$Me_2C_5H_3N$) (**2a**),[12l] [{*o*-((*o*-$MeOC_6H_4)_2P$)$C_6H_4SO_3$}PdCH(CO$_2$Me)CH_2COMe] (**3a**),[11] [(dppe)PdMe(NCMe)][OTf].[67]

General Procedures of Copolymerization of Methyl Acrylate with Carbon Monoxide (Table 1, entry 1). $Pd(dba)_2$ and ligand **1a** (1:1.2 mol ratio) were mixed in a mortar with a pestle. The mixed catalyst (10.7 mg, 0.010 mmol of Pd) were dried in vacuo in a 50 mL-autoclave more than 1.5 h before introducing 1 atm of carbon monoxide. Methyl acrylate (2.5 mL) were then added to the autoclave and the mixture was stirred at 0 °C for 5 min and charged with carbon monoxide at 6.0 MPa. The autoclave was heated to 70 °C and the mixture was stirred. After 20 h, the cooled contents of the autoclave were transferred to a round-bottom flask with CH_2Cl_2 and volatile materials were removed by a rotary evaporator. The remaining solid was dried under vacuum to afford the copolymer. Yield of the copolymer were determined by subtraction of the weight of catalyst (10.7 mg) from the amount of solid product obtained. Molecular weight of the copolymer was determined after filtration of insoluble materials in $CHCl_3$. Reprecipitation and filtration of the crude materials twice from CH_2Cl_2/MeOH or once from CH_2Cl_2/diethyl ether afforded dba-free alternating copolymer.

^{1}H NMR ($CDCl_3$, 500 MHz, Figure S1, top): δ 3.04−3.54 (−CH_2−), 3.60−3.95 (−CO$_2$$CH_3$), 3.96−4.11 (−$CH$(CO$_2$Me)−).

^{13}C NMR ($CDCl_3$, 126 MHz, Figure S2, top): δ 40.2−41.1 (−CH_2−), 52.4−52.8 (−CO$_2$$CH_3$), 52.9 (−$CH$(CO$_2$Me)−), 168.1−168.4 (−CO$_2$$CH_3$), 201.0−201.4 (−$CO$−).

Procedures of Copolymerization of *t*-Butyl Acrylate with Carbon Monoxide (Table 1, entry 11). $Pd(dba)_2$ and ligand **1a** (1:1.2 mol ratio) were mixed in a mortar with a pestle. The mixed catalyst (10.7 mg, 0.010 mmol of Pd) were dried in vacuo in a 50 mL-autoclave more than 1.5 h before introducing 1 atm of carbon monoxide. *t*-Butyl acrylate (2.5 mL) was then added to the autoclave and the mixture was stirred at 0 °C for 5 min and charged with carbon monoxide at 6.0 MPa. The autoclave was heated to 70 °C and the mixture was stirred. After 20 h, the cooled contents of the autoclave were transferred to a round-bottom flask with CH_2Cl_2 and volatile materials were removed by a rotary evaporator. The remaining solid was dried under vacuum to afford the copolymer. Yield of the copolymer were determined by subtraction of the weight of catalyst (10.7 mg) from the amount of solid product obtained. Molecular weight of the copolymer was determined after filtration of insoluble materials in $CHCl_3$. Removal of ligand and dba by reprecipitation failed because of the solubility of the copolymer in MeOH and in diethyl ether.

^{1}H NMR ($CDCl_3$, 400 MHz, Figure S5): δ 1.37−1.55 (−C(CH_3)$_3$), 2.65−3.52 (−CH_2−), 3.69−4.39 (−CH(CO$_2$*t*-Bu)−).

^{13}C NMR ($CDCl_3$, 101 MHz, Figure S6): δ 27.5−28.4 (−C(CH_3)$_3$), 39.2−41.8 (−CH_2−), 53.0−55.8 (−CH(CO$_2$*t*-Bu)−), 81.7−83.2 (−C(CH_3)$_3$), 166.3−167.2 (−CH(CO$_2$*t*-Bu)−), 168.1−168.4 (−CO$_2$$C$($CH_3$)$_3$), 200.8−202.6 (−$CO$−).

General Procedures of Terpolymerization of Methyl Acrylate, Ethylene and Carbon Monoxide Catalyzed by $Pd(dba)_2$ and Phosphonium−Sulfonate (Table 2). $Pd(dba)_2$ and ligand **1a** (1:1.2 mol ratio) were mixed in a mortar with a pestle. The mixed

dx.doi.org/10.1021/ja2003268 |*J. Am. Chem. Soc.* 2011, 133, 6761–6779

catalyst (10.7 mg, 0.010 mmol of Pd) were dried in vacuo in a 50 mL-autoclave more than 1.5 h. To the autoclave were added 2.5 mL of methyl acrylate and then was charged with ethylene quickly at described pressure. Carbon monoxide was quickly charged to the autoclave up to the described total pressure. The autoclave was heated to 70 °C and the mixture was stirred. After 1 h, the cooled contents of the autoclave were transferred to a round-bottom flask with CH_2Cl_2 and volatile materials were removed by a rotary evaporator. The remaining solid was dried under vacuum to afford the terpolymer. Yield of the copolymer were determined by subtraction of the weight of catalyst (10.7 mg) from the amount of solid product obtained. For the reprecipitaion of the terpolymer in entry 1 in Table 2, the obtained materials were dissolved in ca. 1 mL of a mixture of $CDCl_3$/1,1,1,3,3,3-hexafluoro-2-propanol (1:2) was poured into stirring diethyl ether through filtration. The reprecipitated white solid was used for NMR (Figure S10−14, Supporting Information), TG (Figure S21, Supporting Information) and DCS (Figure S22, Supporting Information) analyses. For the terpolymer in entry 2 in Table 2 (NMR: Figure S15, 16, Supporting Information), molecular weight of the copolymer was determined after filtration of insoluble materials in $CHCl_3$.

H/D Exchange of Copoly(Methyl Acrylate-*alt*-CO) (Figure S3, Supporting Information). In a NMR sample tube, 16 mg of copoly(methyl acrylate-*alt*-CO) (0.14 mmol unit, a sample of M_n = 53,000, M_w/M_n = 1.6) was dried under vacuum. After introducing argon, freshly distilled CD_2Cl_2 (0.6 mL) was added to the sample tube and the polymer was dissolved. To a solution of copolymer was added 2.1 mmol of methan-(ol-*d*). After 4 h at ambient temperature, ^{1}H NMR was collected. ^{2}H NMR of the resulting copolymer was also collected in CH_2Cl_2 after removing CD_2Cl_2 and methan-(ol-*d*) under vaccuo.

Reaction of 3a under High Pressure of CO: Spectropcopic Characterization of (*SP*-4-3)-[{*o*-((*o*-MeOC$_6$H$_4$)$_2$P)C$_6$H$_4$SO$_3$}-Pd{COCH(CO$_2$Me)CH$_2$COMe}] (5a).[68] In a globe box, a high pressure-NMR tube was charged with a filtered solution of **3a** (0.25 mmol) in CD_2Cl_2 (0.6 mL). The tube was charged with CO to 6.0 MPa and was kept at room temperature for 3.5 h. Then the NMR data were collected at room temperature. The 3:2 mixture of **5a** and **3a** were observed. (Figure S17, Supporting Information).

NMR data (other than aromatic region) of **3a**[11]: ^{1}H NMR (CD_2Cl_2): δ 1.66−1.79 (m, 1H, PdC*H*), 2.47 (s, 3H, PdCH(CO_2CH_3)(CH_2C(O)C*H*$_3$)), 2.59 (d, J = 18.3 Hz, 1H, PdCH(CO_2CH_3)(C*H*$_2$C(O)CH$_3$)), 2.78 (dd, J = 18.3, 6.0 Hz, 1H, PdCH(CO_2CH_3)(C*H*$_2$C(O)CH$_3$)), 3.26 (s, 3H, PdCH(CO_2C*H*$_3$)(CH_2C(O)CH$_3$)), 3.50 (s, 3H, C*H*$_3$OC$_6$H$_4$), 3.71 (s, 3H, C*H*$_3$OC$_6$H$_4$), 6.89 (dd, J = 8.3, 4.6 Hz, 1H), 6.98−7.07 (m, 2H), 7.14 (dddd, J = 7.6, 7.6, 1.8, 0.9 Hz, 1H), 7.24−7.37 (m, 3H), 7.41−7.49 (m, 1H), 7.52−7.62 (m, 2H), 7.94−8.07 (m, 1H), 8.27 (dd, J = 16.3, 7.3 Hz, 1H); ^{13}C NMR (CD_2Cl_2): δ 27.8 (s, PdCH(CO_2CH_3)(CH_2C(O)C*H*$_3$)), 34.6 (s, PdC*H*), 50.4 (s, PdCH(CO_2CH_3)(C*H*$_2$C(O)CH$_3$)), 50.5 (s, PdCH(CO_2CH_3)(CH_2C(O)C*H*$_3$)), 54.5 (s, C*H*$_3$OC$_6$H$_4$), 55.3 (s, C*H*$_3$OC$_6$H$_4$), 176.9 (s, PdCH(CO_2CH_3)(C*H*$_2$C(O)CH$_3$)), 230.9 (s, PdCH(CO_2CH_3)(CH_2C(O)C*H*$_3$)).; ^{31}P NMR (CD_2Cl_2): δ 19.7.

5a: ^{1}H NMR (CD_2Cl_2, Figure S17, 18, Supporting Information): δ 2.10 (s, 3H, PdCOCH(CO_2CH_3)(CH_2C(O)C*H*$_3$)), 2.65−2.74 (m, 1H, PdCOCH(CO_2CH_3)(C*H*$_2$C(O)CH$_3$)), 2.96−3.06 (m, 1H, PdCOCH(CO_2CH_3)(C*H*$_2$C(O)CH$_3$)), 3.88−3.92 (m, 1H, PdCOC*H*(CO_2CH_3)(CH_2C(O)CH$_3$)), 3.97 (s, 3H, PdCOCH(CO_2C*H*$_3$)(CH_2C(O)CH$_3$)), 3.60 (s, 3H, C*H*$_3$OC$_6$H$_4$), 3.64 (s, 3H, C*H*$_3$OC$_6$H$_4$).; ^{13}C NMR (CD_2Cl_2): δ 28.7 (s, PdCOCH(CO_2CH_3)(CH_2C(O)C*H*$_3$)), 40.6 (s, PdCOCH(CO_2CH_3)(CH_2C(O)CH$_3$)), 54.8 (s, C*H*$_3$OC$_6$H$_4$), 55.1 (s, C*H*$_3$OC$_6$H$_4$), 55.6 (br, PdCOCH(CO_2CH_3)(CH_2C(O)CH$_3$)), 63.7 (d, $^3J_{PC}$ = 15.0 Hz, PdCOC*H*(CO_2CH_3)(CH_2C(O)CH$_3$)), 181.3 (br, PdCOCH(CO_2CH_3)(CH_2C(O)CH$_3$), 202.4 (d, $^2J_{PC}$ = 16.1 Hz, PdCOCH(CO_2CH_3)(CH_2C(O)CH$_3$)), 205.3 (s, PdCOCH(CO_2CH_3)(CH_2C(O)C*H*$_3$)).; ^{31}P NMR (CD_2Cl_2): δ 19.9 (br).

Preparation of [(dppe)PdCH(CO$_2$Me)CH$_2$COMe][OTf] (3c). Under ambient CO pressure, 2.15 g of [(dppe)PdMe(NCMe)][OTf] (3.03 mmol) was dissolved in 30 mL of dichloromethane, and the reaction mixture was stirred for 1 h at rt. To the resulting mixture, 0.80 mL (8.88 mmol, 2.9 equiv) of methyl acrylate in 10 mL of dichloromethane was added and stirred for 5 h at rt. The resulting mixture was filtered through Celite, and the filter cake was washed with CH_2Cl_2. The condensed solution (ca. 40 mL) was poured into diethyl ether (−25 °C) to afford yellow oil. (993 mg, 1.27 mmol, 41.9% yield) The white crystal suitable for X-ray analysis was obtained from THF.; mp: 96−99 °C dec; IR (KBr) cm^{-1}: 1674, 1622, 1437, 1263, 1157, 1039, 637; ^{1}H NMR (CD_2Cl_2, 400 MHz, Figure S19, Supporting Information): δ 1.85−2.00 (m, 1H, PdCH(CO_2CH_3)(CH*H*C(O)CH$_3$)), 2.56−2.87 (m, 4H, PdC*H*, PdCH(CO_2CH_3)(C*H*HC(O)CH$_3$), PC*H*$_2$CH$_2$P), 2.63 (s, 3H, PdCH(CO_2CH_3)(CH_2C(O)C*H*$_3$)), 3.07 (dd, J = 18.3, 6.8 Hz, 1H, PCH$_2$C*H*HP), 3.28 (dd, J = 18.7, 14.1 Hz, 1H, PCH$_2$CH*H*P), 3.14 (s, 3H, CO_2C*H*$_3$), 7.49−7.81 (m, 20H); ^{13}C NMR (CD_2Cl_2, 101 MHz, Figure S20, top, Supporting Information): δ 20.8 (dd, $^3J_{PC}$ = 30, 5 Hz, PdCH(CO_2CH_3)(CH_2C(O)CH$_3$)), 28.4 (d, $^4J_{PC}$ = 2 Hz, PdCH(CO_2CH_3)(CH_2C(O)C*H*$_3$)), 31.0 (dd, $^1J_{PC}$ = 37 Hz, $^2J_{PC}$ = 19 Hz, PCH$_2$CH$_2$P), 48.1 (d, $^1J_{PC}$ = 77 Hz, PdCH), 50.1 (d, $^1J_{PC}$ = 6 Hz, PCH$_2$CH$_2$P), 50.3 (s, CO_2CH_3), 126.1 (d, $^1J_{PC}$ = 58 Hz, 4°), 127.4 (d, $^1J_{PC}$ = 58 Hz, 4°), 128.2 (d, $^1J_{PC}$ = 40 Hz, 4°), 128.7−129.6 (m, CH and 4°), 131.8−132.4 (m, CH), 132.7 (d, J_{PC} = 2 Hz, CH), 134.0 (d, J_{PC} = 13 Hz, CH), 176.7 (d, $^3J_{PC}$ = 6 Hz, PdCH(CO_2CH_3)(CH_2C(O)CH$_3$)), 238.7 (d, $^3J_{PC}$ = 9 Hz, PdCH(CO_2CH_3)(CH_2C(O)CH$_3$)); ^{31}P NMR (CD_2Cl_2, 162 MHz) δ 45.4 (d, $^2J_{PP}$ = 26 Hz), 59.2 (d, $^2J_{PP}$ = 26 Hz); ^{19}F NMR (CD_2Cl_2, 376 MHz) δ −78.8; HRMS-FAB (m/z): [M − $CF_3SO_3^-$]$^+$ calcd for $C_{32}H_{33}O_3P_2Pd$, 633.0940; found, 633.0916.

Reaction of 3c under High Pressure of CO. In a globe box, a high pressure-NMR tube was charged with a filtered solution of **3c** (0.14 mmol) in CD_2Cl_2 (0.6 mL). The tube was charged with CO to 6.0 MPa and was kept at room temperature for 3.5 h. Then the NMR data were collected at room temperature (Figure S20, bottom, Supporting Information). Other than free CO, any change could not be confirmed, at least in carbonyl region.

Theoretical Methods. All geometries of the reactants, intermediates, transition states, and products of the reactions were fully optimized by using Gaussian 03 program,[69] and B3LYP[40] method with combined basis sets (Lanl2dz basis sets and effective core potential for palladium atom[41] and 6-31G(d) basis sets for the other atoms). Harmonic vibration frequency calculations at the same level were performed to verify all stationary points as local minimum (with no imaginary frequency) or transition state (with one imaginary frequency). IRC calculations[70] were also performed to confirm the connectivity between the transition state and the reactant/product. Zero-point energy, enthalpy, and Gibbs free energy at 298.15 K and 1 atm were calculated from the gas-phase harmonic frequencies.

■ ASSOCIATED CONTENT

Supporting Information. Copies of all spectral data, full characterization, and details of theoretical part including Cartesian coordinates and complete citation of ref 69. This material is available free of charge via the Internet at http://pubs.acs.org.

■ AUTHOR INFORMATION

Corresponding Author

nozaki@chembio.t.u-tokyo.ac.jp

Present Addresses

‡Department of Chemistry, Faculty of Science and Technology, Keio University, 3-14-1 Hiyoshi, Kohoku-ku, Yokohama, Kanagawa 223-8522, Japan.

■ ACKNOWLEDGMENT

We are grateful to Assoc. Prof. Y. Nishibayashi and Dr. Y. Miyake at the University of Tokyo for high-resolution FAB-MS analysis of **3c**. We are also grateful to Prof. T. Kato and Dr. T. Yasuda at the University of Tokyo for preliminary XRD analyses. We thank Dr. Zhuofeng Ke at Kyoto University for fruitful discussion on theoretical part. Computer resources for theoretical calculation were mainly provided by the Research Center for Computational Science in the National Institutes of Natural Sciences. This work was supported by the Global COE Program for Chemistry Innovation. A.N. is grateful to the Japan Society for the Promotion of Science (JSPS) for a Research Fellowship for Young Scientists. L.W.C. acknowledges the Fukui Institute Fellowship. This work is in part supported by Japan Science and Technology Agency (JST) with a Core Research for Evolutional Science and Technology (CREST) grant in the Area of High Performance Computing for Multiscale and Multiphysics Phenomena. Partial support by Funding Program for Next Generation World-Leading Researchers, Green Innovation, JSPS, is also acknowledged.

■ REFERENCES

(1) (a) Drent, E.; Budzelaar, P. H. M. *Chem. Rev.* **1996**, *96*, 663–681. (b) Sommazzi, A.; Garbassi, F. *Prog. Polym. Sci.* **1997**, *22*, 1547–1605. (c) Bianchini, C.; Meli, A. *Coord. Chem. Rev.* **2002**, *225*, 35–66. (d) Bianchini, C.; Meli, A.; Oberhauser, W. *Dalton Trans.* **2003**, 2627–2635. (e) Nakano, K.; Kosaka, N.; Hiyama, T.; Nozaki, K. *Dalton Trans.* **2003**, 4039–4050. (f) Durand, J.; Milani, B. *Coord. Chem. Rev.* **2006**, *250*, 542–560. (g) García Suárez, E. J.; Godard, C.; Ruiz, A.; Claver, C. *Eur. J. Inorg. Chem.* **2007**, 2582–2593. (h) Nakamura, A.; Ito, S.; Nozaki, K. *Chem. Rev.* **2009**, *109*, 5215–5244.

(2) *Catalytic Synthesis of Alkene-Carbon Monoxide Copolymers and Cooligomers*; Sen, A., Ed.; Kluwer Academic Publishers: Dordrecht, 2003.

(3) For examples, see: (a) *European Plastics News*; **1995**, *Oct*, 57. (b) Yanai, T.; Okajima, S.; Miyaji, K. Jpn. Kokai Tokkyo Koho 2008,075,219, April 3, 2008.

(4) For examples, see: (a) Milani, B.; Crotti, C.; Farnetti, E. *Dalton Trans.* **2008**, 4659–4663. (b) Kosaka, N.; Hiyama, T.; Nozaki, K. *Macromolecules* **2004**, *37*, 4484–4487. (c) Nozaki, K.; Kosaka, N.; Graubner, V. M.; Hiyama, T. *Macromolecules* **2001**, *34*, 6167–6168. (d) Sen, A.; Jiang, Z. Z.; Chen, J. T. *Macromolecules* **1989**, *22*, 2012–2014.

(5) (a) Sen, A. S.; Jiang, Z. *Macromolecules* **1993**, *26*, 911–915. (b) Kacker, S.; Jiang, Z.; Sen, A. *Macromolecules* **1996**, *29*, 5852–5858. (c) Klok, H. A.; Eibeck, P.; Schmid, M.; Abu-Surrah, A. S.; Möller, M.; Rieger, B. *Macromol. Chem. Phys.* **1997**, *198*, 2759–2768. (d) Nieuwhof, R. P.; Marcelis, A. T. M.; Sudhölter, E. J. R.; Wursche, R.; Rieger, B. *Macromol. Chem. Phys.* **2000**, *201*, 2484–2492. (e) Lee, J. T.; Alper, H. *Chem. Commun.* **2000**, 2189–2190. (f) Moineau, C.; Mele, G.; Alper, H. *Can. J. Chem.* **2001**, *79*, 587–592. (g) Fujita, T.; Nakano, K.; Yamashita, M.; Nozaki, K. *J. Am. Chem. Soc.* **2006**, *128*, 1968–1975. (h) Malinova, V.; Rieger, B. *Macromol. Rapid Commun.* **2005**, *26*, 945. (i) Malinova, V.; Rieger, B. *Biomacromolecules* **2006**, *7*, 2931–2936.

(6) Functionalized bicyclic olefins are also copolymerized with CO, see: (a) Liaw, D. J.; Tsai, J. S.; Sang, H. C. *J. Polym. Sci., Part A: Polym. Chem.* **1998**, *36*, 1785–1790. (b) Safir, A. L.; Novak, B. M. *J. Am. Chem. Soc.* **1998**, *120*, 643–650.

(7) Reactions of methyl acrylate with CO: (a) Ozawa, F.; Hayashi, T.; Koide, H.; Yamamoto, A. *J. Chem. Soc., Chem. Commun.* **1991**, 1469–1470. (b) Dekker, G. P. C. M.; Elsevier, C. J.; Vrieze, K.; van Leeuwen, P. W. N. M.; Roobeek, C. F. *J. Organomet. Chem.* **1992**, *430*, 357–372. (c) Rix, F. C.; Brookhart, M.; White, P. S. *J. Am. Chem. Soc.* **1996**, *118*, 4746–4764. (d) Reddy, K. R.; Chen, C. L.; Liu, Y. H.; Peng, S. M.; Chen, J. T.; Liu, S. T. *Organometallics* **1999**, *18*, 2574–2576. (e) Braunstein, P.; Frison, C.; Morise, X. *Angew. Chem., Int. Ed.* **2000**, *39*, 2867–2870. (f) Braunstein, P.; Durand, J.; Knorr, M.; Strohmann, C. *Chem. Commun.* **2001**, 211–212. (g) Reddy, K. R.; Surekha, K.; Lee, G. H.; Peng, S. M.; Chen, J. T.; Liu, S. T. *Organometallics* **2001**, *20*, 1292–1299. (h) Agostinho, M.; Braunstein, P. *Chem. Commun.* **2007**, 58–60. (i) Agostinho, M.; Braunstein, P. *C. R. Chimie* **2007**, *10*, 666–676. (j) Hamada, A.; Braunstein, P. *Organometallics* **2009**, *28*, 1688–1696.

(8) Reactions of vinyl acetate with CO: (a) Williams, B. S.; Leatherman, M. D.; White, P. S.; Brookhart, M. *J. Am. Chem. Soc.* **2005**, *127*, 5132–5146. See also refs 7d and 7g. Reaction of vinyl chloride with CO:(b) Shen, H.; Jordan, R. F. *Organometallics* **2003**, *22*, 1878–1887. Reaction of acrylonitrile with CO:(c) Wu, F.; Foley, S. R.; Burns, C. T.; Jordan, R. F. *J. Am. Chem. Soc.* **2005**, *127*, 1841–1853. Reaction of vinyl ethers with CO:(d) Chen, C. L.; Chen, Y. C.; Liu, Y. H.; Peng, S. M.; Liu, S. T. *Organometallics* **2002**, *21*, 5382–5385 .

(9) Coordination copolymerizations of these common polar vinyl monomers are one of the most challenging issues in polymer chemistry, see: (a) Boffa, L. S.; Novak, B. M. *Chem. Rev.* **2000**, *100*, 1479–1493. (b) Sen, A.; Borkar, S. *J. Organomet. Chem.* **2007**, *692*, 3291–3299. (c) Berkefeld, A.; Mecking, S. *Angew. Chem., Int. Ed.* **2008**, *47*, 2538–2542. (d) Chen, E. Y. X. *Chem. Rev.* **2009**, *109*, 5157–5214. (e) Ito, S.; Nozaki, K. *Chem. Rec.* **2010**, *10*, 315–325. See also ref 1h.

(10) Kochi, T.; Nakamura, A.; Ida, H.; Nozaki, K. *J. Am. Chem. Soc.* **2007**, *129*, 7770–7771.

(11) Nakamura, A.; Munakata, K.; Kochi, T.; Nozaki, K. *J. Am. Chem. Soc.* **2008**, *130*, 8128–8129.

(12) Methyl acrylate: (a) Drent, E.; van Dijk, R.; van Ginkel, R.; van Oort, B.; Pugh, R. I. *Chem. Commun.* **2002**, 744–745. (b) Kochi, T.; Yoshimura, K.; Nozaki, K. *Dalton Trans.* **2006**, 25–27. (c) Skupov, K. M.; Marella, P. R.; Simard, M.; Yap, G. P. A.; Allen, N.; Conner, D.; Goodall, B. L.; Claverie, J. P. *Macromol. Rapid Commun.* **2007**, *28*, 2033–2038. (d) Guironnet, D.; Roesle, P.; Rünzi, T.; Göttker-Schnetmann, I.; Mecking, S. *J. Am. Chem. Soc.* **2009**, *131*, 422–423. (e) Skupov, K. M.; Hobbs, J.; Marella, P.; Conner, D.; Golisz, S.; Goodall, B. L.; Claverie, J. P. *Macromolecules* **2009**, *42*, 6953–6963. (f) Guironnet, D.; Caporaso, L.; Neuwald, B.; Göttker-Schnetmann, I.; Cavallo, L.; Mecking, S. *J. Am. Chem. Soc.* **2010**, *132*, 4418–4426. Acrylic acid:(g) Rünzi, T.; Fröhlich, D.; Mecking, S. *J. Am. Chem. Soc.* **2010**, *132*, 17690–17691. Vinyl acetate:(h) Ito, S.; Munakata, K.; Nakamura, A.; Nozaki, K. *J. Am. Chem. Soc.* **2009**, *131*, 14606–14607. Acrylonitrile:(i) Kochi, T.; Noda, S.; Yoshimura, K.; Nozaki, K. *J. Am. Chem. Soc.* **2007**, *129*, 8948–8949. (j) Nozaki, K.; Kusumoto, S.; Noda, S.; Kochi, T.; Chung, L. W.; Morokuma, K. *J. Am. Chem. Soc.* **2010**, *132*, 16030–16042. Vinyl Fluoride:(k) Weng, W.; Shen, Z.; Jordan, R. F. *J. Am. Chem. Soc.* **2007**, *129*, 15450–15451. (l) Shen, Z. L.; Jordan, R. F. *Macromolecules* **2010**, *43*, 8706–8708. Vinyl Ethers: (m) Luo, S.; Vela, J.; Lief, G. R.; Jordan, R. F. *J. Am. Chem. Soc.* **2007**, *129*, 8946–8947. Other vinyl polar monomers: (n) Skupov, K. M.; Piche, L.; Claverie, J. P. *Macromolecules* **2008**, *41*, 2309–2310. (o) Borkar, S.; Newsham, D. K.; Sen, A. *Organometallics* **2008**, *27*, 3331–3334. (p) Bouilhac, C.; Runzi, T.; Mecking, S. *Macromolecules* **2010**, *43*, 3589–3590. See also ref 1h. Allyl monomers: (q) Ito, S.; Kanazawa, K.; Munakata, K.; Kuroda, J.; Okumura, Y.; Nozaki, K. *J. Am. Chem. Soc.* **2011**, *133*, 1232–1235.

(13) For some early patents, see:(a) Murray, R. E. U.S. Patent 4,689,437, August 25, 1987. (b) van Doorn, J. A.; Drent, E.; van Leeuwen, P. W. N.; Meijboom, N.; van Oort, A. B.; Wife, R. L., Eur. Pat. Appl. 0,280,380, August 31, 1988. (c) Bradford, A. M.; Van Leeuwen, P. W. N.; Wullink-Schelvis, A. M. WO Patent Application 9324553, December 9, 1993. See also ref 1h.

(14) For the mechanism of the formation of the linear polyethylene catalyzed by Pd phosphine−sulfonate complexes, see: (a) Noda, S.; Nakamura, A.; Kochi, T.; Chung, L. W.; Morokuma, K.; Nozaki, K. *J. Am. Chem. Soc.* **2009**, *131*, 14088–14100. Very recently, Jordan proposed another possible *cis*/*trans* isomerization mechanism: (b) Conley, M. P.; Jordan, R. F. *Angew. Chem. Int. Ed.* **2011**, *50*, 3744–3746.

(15) (a) Drent, E.; van Dijk, R.; van Ginkel, R.; van Oort, B.; Pugh, R. I. *Chem. Commun.* **2002**, 964–965. (b) Hearley, A. K.; Nowack,

R. A. J.; Rieger, B. *Organometallics* **2005**, *24*, 2755–2763. (c) Newsham, D. K.; Borkar, S.; Sen, A.; Conner, D. M.; Goodall, B. L. *Organometallics* **2007**, *26*, 3636–3638. (d) Bettucci, L.; Bianchini, C.; Claver, C.; Suarez, E. J. G.; Ruiz, A.; Meli, A.; Oberhauser, W. *Dalton Trans.* **2007**, 5590–5602. (e) Luo, R.; Newsham, D. K.; Sen, A. *Organometallics* **2009**, *28*, 6994–7000.

(16) Theoretical calculations of nonalternating copolymerization of ethylene with CO: (a) Haras, A.; Michalak, A.; Rieger, B.; Ziegler, T. *J. Am. Chem. Soc.* **2005**, *127*, 8765–8774. (b) Haras, A.; Michalak, A.; Rieger, B.; Ziegler, T. *Organometallics* **2006**, *25*, 946–953.

(17) When $Pd_2(dba)_3 \cdot CHCl_3$ was used, the activity and the molecular weight were enhanced (activity, 3.0 $g \cdot mmol^{-1} \cdot h^{-1}$; M_n, 64 000; M_w/M_n, 4.3). For the preparation of $Pd(dba)_2$ and $Pd_2(dba)_3 \cdot CHCl_3$, see: Ukai, T.; Kawazura, H.; Ishii, Y.; Bonnet, J. J.; Ibers, J. A. *J. Organomet. Chem.* **1974**, *65*, 253–266.

(18) Slight amount of Pd black was observed after the reaction. See also ref 39.

(19) The complex **2a** can copolymerize ethylene and MA with low MA ratio (unpublished resuls, see also references[12d] for a result by a pyridine adduct complex). Considering the copolymerization of MA with CO proceeds in alternating fashion, coordination of MA should occur in each catalytic cycle. Thus, MA/CO copolymerization should be more sluggish than ethylene/CO copolymerization with low MA ratio.

(20) Recently, the reactivity of methyl methacrylate with Pd phosphine−sulfonate complex was studied in detail, see: Runzi, T.; Guironnet, D.; Göttker-Schnetmann, I.; Mecking, S. *J. Am. Chem. Soc.* **2010**, *132*, 16623–16630.

(21) Hauptman, E.; Saboetienne, S.; White, P. S.; Brookhart, M.; Garner, J. M.; Fagan, P. J.; Calabrese, J. C. *J. Am. Chem. Soc.* **1994**, *116*, 8038–8060.

(22) Nagashima, H.; Itonaga, C.; Yasuhara, J.; Motoyama, Y.; Matsubara, K. *Organometallics* **2004**, *23*, 5779–5786.

(23) As often observed in other γ-polyketones such as poly(propylene-*alt*-CO), spiroketal repeat units instead of ketone units can be also generated. After slow evaporation for 4 month from the $CDCl_3$ solution of the poly(methyl acrylate-*alt*-CO), ^{13}C NMR showed broad signal at 110.6−115.5 ppm which is typical region for spiro quarternary carbon.

(24) Nozaki, K.; Sato, N.; Takaya, H. *J. Am. Chem. Soc.* **1995**, *117*, 9911–9912.

(25) Enol form of the β-ketoester was not detected from the ^1H NMR spectrum.

(26) This epimerization rate was similar to that of the corresponding small molecule: when methyl-2-methyl-3-oxopentanoate ($EtCOCH(CO_2Me)CH_3$) was treated with 15 equivalents of MeOD in CD_2Cl_2, 25% of the methine protons were exchanged with deuterium after 4 h at room temperature.

(27) If the stereochemistry of poly(methyl acrylate-*alt*-CO) is thermodynamically controlled and the split signals at low temperature are originated from the fluctuation of higher-order structure, it is still unclear whether the regiochemistry of poly(*t*-butyl acrylate-*alt*-CO) is controlled or not.

(28) For the comparison of the reactivity of MA and ethylene, see: (a) Mecking, S.; Johnson, L. K.; Wang, L.; Brookhart, M. *J. Am. Chem. Soc.* **1998**, *120*, 888–899. (b) Kang, M. S.; Sen, A.; Zakharov, L.; Rheingold, A. L. *J. Am. Chem. Soc.* **2002**, *124*, 12080–12081. (c) Popeney, C. S.; Guan, Z. B. *J. Am. Chem. Soc.* **2009**, *131*, 12384–12393. (d) Srebro, M.; Mitoraj, M.; Michalak, A. *Can. J. Chem.* **2009**, *87*, 1039–1054 and references cited therein. See also refs 56 and 57.

(29) Recently, we reported terpolymerization of styrene/vinyl acetate/CO and styrene/methyl acrylate/CO by using the same catalyst, see: Kageyama, T.; Ito, S.; Nozaki, K. *Chem. Asian J.* **2011**, *6*, 690–697.

(30) AbuSurrah, A. S.; Wursche, R.; Rieger, B. *Macromol. Chem. Phys.* **1997**, *198*, 1197–1208.

(31) However, preliminary XRD analyses showed tiny signals for poly(MA-*alt*-CO) and poly(CO-*alt*-(ethylene; MA)). The results indicate the possibility of being crystalline polymer. Further investigations for the physical properties are in progress.

(32) It is known that the activity for the copolymerization of ethylene with CO is higher when diphenylphosphinopropane (DPPP) is used than that of DPPE (ref 1a). However, we chose DPPE for the discussion because of the decreased degrees of freedom of the ligand for the theoretical study. Note that the calculated energy required for the rate-determining step was 38.9 kcal/mol by utilizing DPPP as a ligand, which is even higher than that of DPPE. See section 7.

(33) Drent et. al. patented the terpolymerization of MA/ethylene/CO by using the combination of $Pd(OAc)_2$ and DPPE, see: Drent, E. Eur. Pat. Appl. 0,272,727, June 29, 1988.

(34) Our calculation suggested that the relative stabilities of the product derived from homolytic cleavage of Pd−C bond of $\mathbf{A_{cis}}$ and $\mathbf{A_{PP}}$ are 55.5/39.0 and 58.2/40.6 kcal/mol respectively. See also ref 9b for the discussion of homolytic cleavage of Pd−$CH(CO_2Me)$R bond.

(35) Jordan and co-workers described in ref 8b that five-membered chelate complexes with α-Cl substituent ($[N-N]PdCHClCH_2COCH_3$) were inert to the insertion of CO. The Pd−C and Pd−O bond distances, determined by X-ray diffraction, are at the short end of the ranges observed in the analogous non-halogenated five-membered chelate complexes.

(36) It is widely known that OH^- ligand is classified as weak *trans* effect/influence ligand, see: (a) *The Organometallic Chemistry of the Transition Metals*, 4th ed; Crabtree, R, Ed.; Wiley: New York, 2005. (b) *Organotransition Metal Chemistry From Bonding to Catalysis* Hartwig, J., Ed.; University Science Books: Herndon, VA, 2009.

(37) The bulkier *o*-$CH_3OC_6H_4$ group on phosphorus atom in **3c** makes this comparison imperfect.

(38) Because 2D NMR spectra were not applicable under the high pressure conditions, these signals were characterized by comparisons to the literature. Note that our high-pressure NMR apparatus is not applicable at higher temperature.

(39) While taking ^{13}C NMR, the palladium complexes gradually decomposed to result in the formation of some Pd black.

(40) (a) Becke, A. D. *J. Chem. Phys.* **1993**, *98*, 5648–5652. (b) Lee, C.; Yang, W.; Parr, R. G. *Phys. Rev. B* **1988**, *37*, 785–789.

(41) Hay, P. J.; Wadt, W. R. *J. Chem. Phys.* **1985**, *82*, 270–283.

(42) Comparison of B3LYP/6-31G* with Lanl2dz and B3LYP/6-311+G** with SDD +f is described in Supporting Information. Because the copolymerization was conducted under neat condition, PCM calculation was not performed to avoid inappropriate discussion. Largely, B3LYP/6-31G* with Lanl2dz in gas phase sufficiently match with our experiments. See also ref 14.

(43) For example of the theoretical studies employing other unsymmetrical bidentate ligands in coordination−insertion polymerizations, see: (a) Nozaki, K.; Sato, N.; Tonomura, Y.; Yasutomi, M.; Takaya, H.; Hiyama, T.; Matsubara, T.; Koga, N. *J. Am. Chem. Soc.* **1997**, *119*, 12779–12795. (b) Nozaki, K.; Komaki, H.; Kawashima, Y.; Hiyama, T.; Matsubara, T. *J. Am. Chem. Soc.* **2001**, *123*, 534–544. (c) Deubel, D. V.; Ziegler, T. *Organometallics* **2002**, *21*, 4432–4441. (d) Michalak, A.; Ziegler, T. *Organometallics* **2003**, *22*, 2069–2079. (e) Yang, S. Y.; Szabo, M. J.; Michalak, A.; Weiss, T.; Piers, W. E.; Jordan, R. F.; Ziegler, T. *Organometallics* **2005**, *24*, 1242–1251.

(44) The alkyl chains of $\mathbf{B_{cis}}$ and $\mathbf{B_{trans}}$ have different conformations because we adopted the most stable structures for these intermediates (See Supporting Information). For example, internal ketone carbonyl oxygen coordinates to the Pd center at apical position in $\mathbf{B_{trans}}$ while not in $\mathbf{B_{cis}}$ to avoid the steric repulsion with Ph groups. It should be noted that $\mathbf{B_{cis}}$ was less stable in energy than $\mathbf{B_{trans}}$ regardless of the ketone coordination.

(45) (a) Dahlenburg, L.; Vondeuten, K.; Kopf, J. *J. Organomet. Chem.* **1981**, *216*, 113–127. (b) Manojlovic-Muir., L. J.; Muir, K. W. *Inorg. Chim. Acta* **1974**, *10*, 47–49. See also ref 16.

(46) Dias, P. B.; Depiedade, M. E. M.; Simoes, J. A. M. *Coord. Chem. Rev.* **1994**, *135*, 737–807.

(47) Although a σ^* orbital of the S−O single bond might be in the suitable position to overlap the filled d_π orbitals of a Pd center, the coefficient of its vacant orbital should be mainly on the S atom. In addition, such an interaction was not found in the molecular orbitals from HOMO-5 to LUMO+10 of $\mathbf{B_{trans}}$. Instead, the repulsion between lone pairs on the oxygen atom of a sulfonate group and d_π orbitals of a Pd

center can be confirmed in several molecular orbitals. For a related study of the orbital of H-SO_3-CCH, see: Stang, P. J.; Crittell, C. M.; Arif, A. M.; Karni, M.; Apeloig, Y. *J. Am. Chem. Soc.* **1991**, *113*, 7461–7470.

(48) It was expected from these calculations that the IR spectrum of these carbonyl complexes would give us important implication. Thus, we conducted some experiments to take IR spectrum of carbonyl complexes, however, carbonyl complexes were not isolable and the signals in IR spectrum under CO atmosphere were too complicated to assign for both Pd phosphine−sulfonate and Pd dppe systems.

(49) (a) Weinhold, F.; Carpenter, J. E. In *The Structure of Small Molecules and Ions*; Naaman, R., Vager, Z., Eds.; Plenum: New York, 1988; pp 227−236. (b) Reed, A. E.; Curtiss, L. A.; Weinhold, F. *Chem. Rev.* **1988**, *88*, 899–926.

(50) Between $\mathbf{B_{cis}}$ and **Bmed**, we could find **TS($\mathbf{B_{cis}}$−Bmed)** and it only requires 1.3 /1.9 kcal/mol from **Bmed**. We assume that the other transition states, namely, **TS($\mathbf{A_{cis}}$−Amed)**, **TS(Amed−$\mathbf{A_{trans}}$)**, and **TS(Bmed−$\mathbf{B_{trans}}$)** are barrierless or have a very low barrier. In fact, some energy (E+ZPE) plots of single point calculation suggested that there is no barrier between **Bmed** and $\mathbf{B_{trans}}$.

(51) (a) Zuidema, E.; Bo, C.; van Leeuwen, P. W. M. N. *J. Am. Chem. Soc.* **2007**, *129*, 3989–4000. (b) Frankcombe, K. E.; Cavell, K. J.; Yates, B. F.; Knott, R. B. *Organometallics* **1997**, *16*, 3199–3206. (c) Frankcombe, K. E.; Cavell, K. J.; Yates, B. F.; Knott, R. B. *J. Phys. Chem.* **1996**, *100*, 18363–18370. (d) Cross, R. J. *Chem. Soc. Rev.* **1985**, *14*, 197–223. (e) Anderson, G. K.; Cross, R. J. *Acc. Chem. Res.* **1984**, *17*, 67–74.

(52) Similar transition states were expected in ethylene/CO copolymerization, see: (a) Margl, P.; Ziegler, T. *J. Am. Chem. Soc.* **1996**, *118*, 7337–7344. (b) Margl, P.; Ziegler, T. *Organometallics* **1996**, *15*, 5519–5523.

(53) Other possible pathways, such as a transition state between $\mathbf{A_{cis}}$ and $\mathbf{A_{trans}}$ involving CO and a direct insertion of CO at apical position could not be found.

(54) The six-membered chelate structures with ketone coordination were also found with slight differences in energy: **$\mathbf{C_{cis}$-keto}** (−8.4/0.8 kcal/mol), **$\mathbf{C_{trans}$-keto}** (2.9/10.6 kcal/mol), **TS($\mathbf{C_{cis}$-keto−$\mathbf{C_{trans}$-keto)}** (9.0/16.9 kcal/mol), **$\mathbf{C_{PP}$-keto}** (−3.2/5.1 kcal/mol). Further coordination of CO instead of the internal carbonyl coordination was also considered (i.e. Pd(CO)[$COCH(CO_2Me)CH_2COMe$]): $\mathbf{H_{cis}}$ ($\mathbf{C_{cis}}$ + CO, −17.2/0.3 kcal/mol), $\mathbf{H_{trans}}$ ($\mathbf{C_{trans}}$ + CO, −19.2/−1.2 kcal/mol), and $\mathbf{H_{PP}}$ ($\mathbf{C_{PP}}$ + CO, −12.6/4.5 kcal/mol) (for each structure, see Supporting Information). Coordination of CO to acylpalladium complexes in the reaction media was also suggested in the copolymerization of ethylene with CO (Mul, W. P.; Oosterbeek, H.; Beitel, G. A.; Kramer, G. J.; Drent, E. *Angew. Chem., Int. Ed.* **2000**, *39*, 1848–1851). Although the calculated relative Gibbs free energies of $\mathbf{B_{trans}}$, **$\mathbf{C_{cis}$-keto}**, $\mathbf{H_{cis}}$ and $\mathbf{H_{trans}}$ are comparable to $\mathbf{A_{cis}}$ (**3a**) and **$\mathbf{C_{cis}$(5a)**, they were not observed in the experiment in Figure 5. This inconsistence between experiments and calculation may be attributed to the less inaccurate estimation of entropy.

(55) The internal ketone coordination to the cationic Pd center from the apical position can stabilize $\mathbf{B_{PP}}$ and **TS($\mathbf{B_{PP}}$−$\mathbf{C_{PP}}$)**. For example, $\mathbf{B_{PP}}$ became unstable for 3.9 kcal/mol without ketone coordination. This tendency is contrastive to the neutral Pd phosphine−sulfonate case whose stabilities are not so influenced by the existence of internal ketone coordination. See also ref 44.

(56) (a) von Schenck, H.; Strömberg, S.; Zetterberg, K.; Ludwig, M.; Åkermark, B.; Svensson, M. *Organometallics* **2001**, *20*, 2813–2819. (b) Szabo, M. J.; Jordan, R. F.; Michalak, A.; Piers, W. E.; Weiss, T.; Yang, S. Y.; Ziegler, T. *Organometallics* **2004**, *23*, 5565–5572. (c) Philipp, D. M.; Muller, R. P.; Goddard, W. A.; Storer, J.; McAdon, M.; Mullins, M. *J. Am. Chem. Soc.* **2002**, *124*, 10198–10210.

(57) (a) Michalak, A.; Ziegler, T. *J. Am. Chem. Soc.* **2001**, *123*, 12266–12278. (b) Michalak, A.; Ziegler, T. *Organometallics* **2003**, *22*, 2660–2669. (c) Haras, A.; Anderson, G. D. W.; Michalak, A.; Rieger, B.; Ziegler, T. *Organometallics* **2006**, *25*, 4491–4497.

(58) Comparative studies by theoretical calculations of the preference between 2,1- and 1,2-insertion with vinyl acetate/CO copolymerization are now in progress. See ref 10.

(59) The transition state for MA coordination to complexes **$\mathbf{C_{cis}$-keto**, **$\mathbf{C_{trans}$-keto**, $\mathbf{H_{cis}}$ or $\mathbf{H_{trans}}$ could not be located either. See ref 54.

(60) Shultz, C. S.; Ledford, J.; DeSimone, J. M.; Brookhart, M. *J. Am. Chem. Soc.* **2000**, *122*, 6351–6356.

(61) It is also well-established that the double insertion of CO is thermodynamically disfavorable. In the case of Pd phosphine−sulfonate catalysts, double CO insertion from Pd(CO)COMe (can be expressed as $\mathbf{^*H_{trans}}$, see ref 54) requires a barrier of 20.7/20.9 kcal/mol and the product is 13.9/15.1 kcal/mol above the starting material. Considering much more stable product after the sequential insertion of CO and MA ($\mathbf{A_{cis}}$, −7.9/−2.4 kcal/mol on the basis of Pd(CO)COMe), double CO insertion is unlikely. See also: (a) ref 1. (b) Chen, J. T.; Sen, A. *J. Am. Chem. Soc.* **1984**, *106*, 1506–1507.

(62) Although $\mathbf{B_{trans}}$ and $\mathbf{C_{cis}}$ are lower in energy than $\mathbf{A_{cis}}$, we employed $\mathbf{A_{cis}}$ as a standard for the following discussion because the differences are quite slight and within the error of the calculation. See also ref 54.

(63) Hammond, G. *J. Am. Chem. Soc.* **1955**, *77*, 334.

(64) Some studies of novel ligands inspired by phosphine−sulfonate ligands, see: (a) Reisinger, C. M.; Nowack, R. J.; Volkmer, D.; Rieger, B. *Dalton Trans.* **2007**, 272–278. (b) Nagai, Y.; Kochi, T.; Nozaki, K. *Organometallics* **2009**, *28*, 6131–6134. (c) Zhu, H. J.; Ziegler, T. *Organometallics* **2009**, *28*, 2773–2777.

(65) Some applications of phosphine−sulfonate ligands to the other organic reactions, see: (a) Schultz, T.; Pfaltz, A. *Synthesis* **2005**, 1005–1011. (b) Garcia Suarez, E. J.; Ruiz, A.; Castillón, S.; Oberhauser, W.; Bianchini, C.; Claver, C. *Dalton Trans.* **2007**, 2859–2861. (c) Bettucci, L.; Bianchini, C.; Meli, A.; Oberhauser, W. *J. Mol. Catal. A: Chem.* **2008**, *291*, 57. (d) Sundararaju, B.; Achard, M.; Demerseman, B.; Toupet, L.; Sharma, G. V. M.; Bruneau, C. *Angew. Chem., Int. Ed.* **2010**, *49*, 2782–2785.

(66) Pangborn, A. B.; Giardello, M. A.; Grubbs, R. H.; Rosen, R. K.; Timmers, F. J. *Organometallics* **1996**, *15*, 1518–1520.

(67) Dekker, G. P. C. M.; Elsevier, C. J.; Vrieze, K.; Vanleeuwen, P. W. N. M. *Organometallics* **1992**, *11*, 1598–1603.

(68) "SP-4-3" represents the stereochemical information of the square planar complex. See: IUPAC *Nomenclature of Inorganic Chemistry, Recommendations 2005*; Blackwell Scientific Publications: Oxford, 2005.

(69) Frisch, M. J. et al. *Gaussian 03*, Revision C02; Gaussian, Inc.: Wallingford, CT, 2007.

(70) (a) Gonzalez, C.; Schlegel, H. B. *J. Chem. Phys.* **1989**, *90*, 2154–2161. (b) Gonzalez, C.; Schlegel, H. B. *J. Phys. Chem.* **1990**, *94*, 5523–5527.